Towards high aspect ratio silica coated gold nanorods capable of smectic ordering for Surface Enhanced Raman spectroscopy

Thomas Jan Noordman

Supervised by:

Harith Gurunarayanan MSc

Prof. Dr. Alfons van Blaaderen

Dr. Arnout Imhof

SCMB group at Debey institute for University Utrecht

Master thesis for Nanomaterial science

Abstract

Raman Spectroscopy is used to investigate the vibrational energy modes of molecules. However, the Raman signals are 10_{10} till 10_{15} times weaker than typical fluorescence spectroscopy. Surface Enhanced Raman Scattering (SERS) is a methodology that uses colloidal metal nanoparticles with plasmonic properties to boost the Raman signal by orders of magnitude via electromagnetic enhancement.

Silver particles would give the strongest enhancement. However, gold is used more often as it chemical more stable and there is an wider variety of available shapes. The shape of the nanoparticle also strongly influences the enhancement factor. The local enhancement will be stronger at strong curvatures due to the near field effecs of the plasmon resonance. Because of this, a rod shape is a good shape to use. These nanorods will have a strong enhancement at the tips. Further, if the local electromagnetic fields of nanoparticles overlap, they create so called hotspots, increasing the electromagnetic enhancement. By configuring the gold nanorods in an end-to-end orientation would, in theory, create the strongest enhancement, because of the linking of the hotspot. A novel way to do this is by creating a smectic-ordered liquid crystal. In a smectic ordered system, the tips of the rods are aligned as the rods are oriented the same way and layer by layer. When rods have an aspect ratio (length divided by width) of at least 4.1 to 1, then rods can form this smectic ordering through self-assembly.

The gold nanorods were coated with mesoporous silica oxide. This improves thermal stability and reduces toxicity. Further, the silica layer will prevent aggregation of the gold nanorods. To do this, the silica layer needs a certain thickness. How thick depends on the aspect ratio of the gold nanorod. However, the thicker the silica layer, the lower the aspect ratio. It was calculated that using a gold rod with an aspect ratio of at least 6.9 gives enough room to create a thick enough silica layer to prevent the aggregation of the gold nano rods without silica layer becoming to thick that the aspect ratio of the total particle would be lower than 4.1.

In this thesis, gold nanorods were achieved with various aspect ratios ranging from 2.2 to 5.6 via the Ye & Murray's method. Using the Chang & Murphy's method gold nanorods with an aspect ratio up to 8.5 could be synthesized. However, due to the ageing of $NaBH_4$ or bad stock solutions of NaOH, it was impossible to create such a high aspect ratio at the end of the thesis.

Controlling the thickness of the silica layer by adjusting the concentration of tetraethyl orthosilicate (TEOS) is difficult. Another way to do this is by adding 2-(Methoxy(polyethyleneoxy)propyl)trimethoxysilane (PEG-silane). By adding this chemical at different time intervals during the silica shell formation, the silica-coated gold nanorods could be created with various thicknesses. Further, it is shown that dissolving TEOS in methanol resulted in thinner and smoother silica layers. Further, it is shown that the concentration and the dimension of the gold nanorod strongly influence the formation of the silica layer. In the end, a silica-coated gold nanoparticle was created with an aspect ratio of 3.9.

Contents

1 Introduction

1.1 Raman spectroscopy

Among chemist it is well known that the basis for many spectroscopy techniques is the absorption and excitation of photons [1]. One of these techniques is Raman spectroscopy, which is used to determine the vibrational energy modes of a molecule or atom. The vibrational states correspond to rotations and vibrations of atoms inside of the molecule. Therefore, Raman spectroscopy is used for various applications [1] that include chemical bonds [2], particle interactions [3] and identifying molecules [4]. It finds applications in many fields such as art history [5], geology [3], forensics science [6] and pharmaceutical studies [7].

To be able to give an explanation on how Raman spectroscopy works and how it differs from other spectroscopy techniques, one has to understand how optical extinction spectroscopy works. As is well known, electrons surrounding an atom have a quantised amount of energy, called an energy state. For electrons to go from one state to another, a precise amount of energy is needed. It is impossible for electrons to have an energy level between two electron states. Photons, which can be seen as packages of energy, can excite an electron. Here the energy of the photon is absorbed in the electron, causing the electron to go to a higher state. Since the electron can't have energy between two states, only photons with an exact right amount of energy can take an electron to the excited state. This process is called absorption (see figure 1.1). As electrons want to be in the lowest energy state possible, this excited state is unstable. To go back to the lowest state (the ground state), the electron has to lose the energy again by emitting a photon again or in the form of heat. The process of first absorbing a photon and then emitting a photon is called luminescence and is schematically shown in figure 1.1 [1]. Important here is to realise that this is a two-step process.

It is possible that one photon is absorbed and an other one is emitted at the same time. This is called scattering. This can happen in two ways. One way is elastic scattering, where all the energy of the absorbed photon is transferred to the emitted photon. This is called Rayleigh scattering. Here the energy of the molecule doesn't change as all energy of one photon is directly transported to the other photon.

The other way is inelastic scattering. Here there is a difference in the energy of the absorbed photon and the emitted photon (usually the energy of the absorbed photon is higher than that of the emitted photon). As energy cannot just disappear, the difference in energy goes to (or comes from) the molecule. This is called Raman scattering (see figure 1.1). If the energy of the scattered photon is lower than that of the absorbed photon, the molecule gains some energy. This is called Stokes Raman scattering. If the

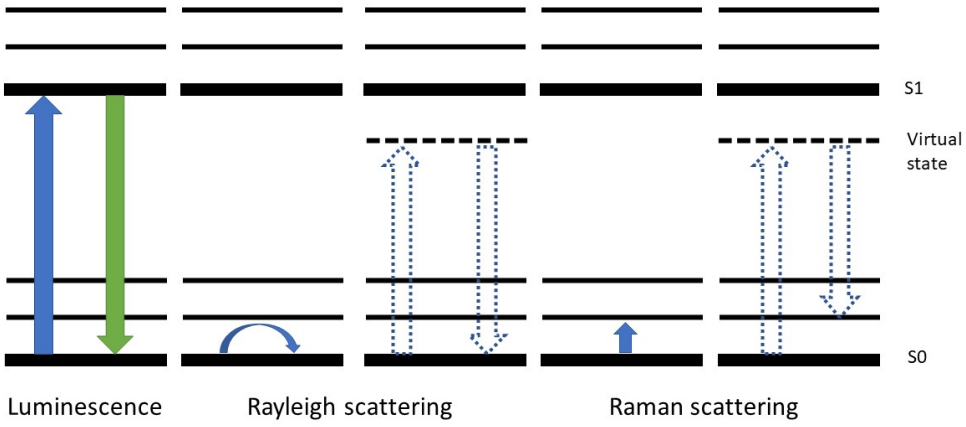

Figure 1.1: A simplified Jablonski diagram showing the energy levels of the ground state, S0, and first excited state, S1, (bold lines) including vibrational energy levels (thinner lines). From left to right it is showing: luminescence, both showing absorption of a photon in blue and excitation in green; Rayleigh scattering with on the left the real process and on the right the two-step approach via a virtual state; and Raman scattering (Stokes Raman in this case) with on the left the real process and on the right the two-step approach via an virtual state. Source: self-made

energy of the scattered photon is higher than that of the absorbed photon, then the molecule loses some energy. This is called anti-Stokes Raman scattering. It is evident that for anti-Stokes Raman scattering the molecule can not be in the ground state before the scattering as then there isn't any energy to take from the molecule. However, since molecules are in the ground state most of the time, Stoke Raman scattering happens way more often than anti-Stokes scattering. [1]

As the energy difference between the photons can be quite small, Raman scattering is able to excite the molecule in the vibrational energy levels. For luminescence to do this, the wavelength needs to be high enough so the energy of the photons becomes low enough. For this, the wavelength needs to be in the IR regime and so it is called IR-luminescence. IR-luminescence and Raman both are used to investigate these vibrational energies. However, because their processes are different, they give different information about these states [1].

Because in scattering the process of absorbing and emitting electrons happens simultaneously, the electrons are actually never in the excited state (which is thus different than in the case for luminescence). Because of this, the energy the absorbed photon has doesn't need to match the precise energy difference between the two states. When one looks at scattering as a two-step process (which is thus strictly speaking false, but can help with understanding the process) then the energy 'state' the molecule would go to in the 'absorption' step is called a virtual state. The energy of the virtual state can be less than the energy required to go to the first excited state. These virtual processes are drawn in figure 1.1 as dotted arrows [1].

Even though Raman spectroscopy is a powerful tool for the identification of materials and quantitative analysis [8], one of the biggest drawbacks of Raman spectroscopy is that the signal is pretty weak. Only 1 in 10^4 photons is scattered [9]. And most scattering is Rayleigh scattering and not Raman scattering [1]. Only one in every 10^6 to 10^{10} photons produced Raman scattering [8, 10]. The cross-section for Raman scattering is 10^{10} to 10^{15} times smaller than the typical fluorescence cross-section of dye molecules [11]. Thus the overall intensity of the Raman signal is way lower than compared to fluorescence. Because of this, large amounts of the material are needed to measure the Raman spectrum of a certain compound. However, this is not always available [10]. A solution for this problem is to somehow enhance the Raman signal. How one could do this, will be discussed in the next section.

1.2 Enhancing the Raman signal

To find a way to enhance the Raman signal, it could be useful to look into the selection rules for Raman spectroscopy. These are an important part of spectroscopy. These rules dictate which transitions between energy states are allowed and which transitions aren't, or in other words: are likely to happen and which are likely not to happen. An important selection rule for Raman scattering is that the scattering can only happen if the photons are able to change the magnitude of dipole of the molecule [1]. The bigger this change, the stronger the Raman signal [9]. Electric polarizability says something about how strong the electric dipole moment changes in an electric field [12]. It is defined as

$$\alpha = \frac{\mu}{E_{loc}} \tag{1.1}$$

Or in words; the polarizability (α) is how much the magnitude of the dipole (μ) changes in a localized electric field (E_{loc}) [12]. Note that polarizability says something about the change in a dipole moment and not something about the dipole moment itself. Apolar compounds, such as alkenes, are much more polarizable than polar compounds such as water. Because water has already a big dipole moment, it will not change much as the local electric field changes. While an alkene doesn't have (a big) permanent dipole. So a small change in the dipole results in a lot of polarizability [13].

For Raman spectroscopy, this means that vibrational bonds that have a large change in dipole when excited will have a large intensity (such as C=C double bonds), while vibrations with a high polarity will not (such as an O-H bond). A nice consequence of this is that Raman spectroscopy can be measured while the molecules are dissolved in water, without much interference from the water itself [13].

Equation 1.1 gives an idea of how the Raman signal could be enhanced; either a larger E_{loc} or larger α. This is the basis for two types of enhancement; electromagnetic enhancement (EM) which is aimed at

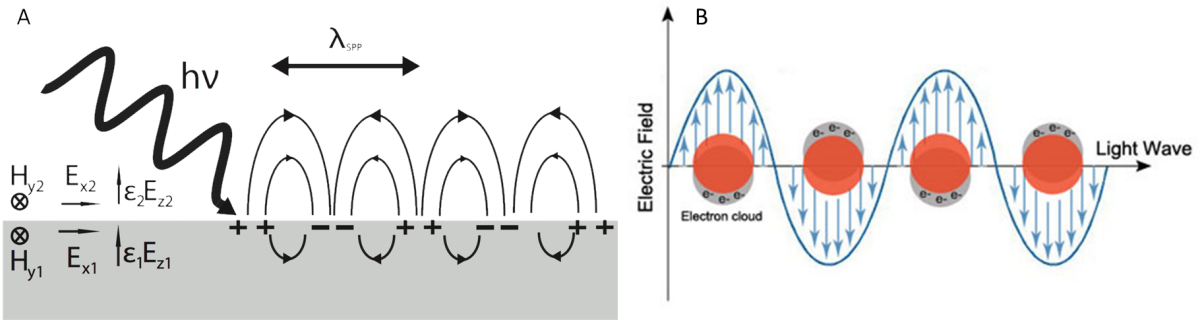

Figure 1.2: A schematic drawing showing the interaction of an incoming light wave and a plasmonic metal. The image on the left (A) shows how it works for bulk metals, where an incoming light wave will create a propagating wave on the edge of the metal. (B) shows how it works for spheres which are smaller than the wavelength of the light wave. Here the light wave will not hit the particle directly, but the electromagnetic properties of the light wave will influence the electron cloud density. Source images a: [17], b: [18]

increasing the local electric field and chemical enhancement, which is aimed at increasing the polarizability [14].

Chemical enhancement encompasses a lot of different types of enhancements which all deal with specific chemical interactions, such as charge-transfer transitions between a metal electronic state of a transmitter and the organic electron states of the molecule. It is mainly focused on using specific bonds to increase the polarizability. Further explanation of the chemical enhancement would be out of the scope of this thesis. For the interested reader, I would like to refer to the literature paper by Ding et al. from 2017 [15].

For electromagnetic enhancement, the local electric field is enhanced [16]. The way to enhance the electric field is through an interaction between metal nanostructures and light. Here these nanostructures are used as an optical antenna [11]. For a deeper understanding of how this works, we first have to understand plasmon resonance.

Plasmon Resonance

Plasmon resonance is the reason that some metal nanoparticles have bright colours [16]. These bright colours of metal nanoparticles have been known to mankind for centuries [19]. The Lycurgus cup (see figure A.1) is an example from the fourth century which uses gold and silver nanoparticles to get optical characteristics. Another example is the colourful stained glass windows of medieval churches all across Europe [19]. Research about where these colours come from is at least as old as Faraday in the 19th century [19, 20], but the first quantitative description of the interaction between light and metal seems to be from Gustav Mie in 1908 [19, 21].

The general theory goes as follows: instead of electron being close to their atoms, for bulk metals electrons can be approximated as being free to travel through the whole material [16]. The electron density of a bulk metal can be approximated as a constant (without outside interactions). Light, which consists of an electromagnetic wave will interact with this electron density. When a photon hits the bulk metal at a certain spot, this will decrease the electron density locally. Since the material will try to balance itself, there will be a slightly negative charge somewhere else. If a wavelength hits with a specific wavelength, this balancing of positive and negative charges can result in an oscillation of the free electrons in the bulk metal, forming a propagating wave. This wave is called the surface plasmon oscillation. The effect that photons have on the electron density in bulk metals is drawn schematically in figure 1.2A [14, 16].

For nanoparticles, this plasmon response works slightly differently. If the particles become (much) smaller than the wavelength of light - which is between 380 and 750 nm for visible light - then an entire oscillation of a light wave can surround a particle. Due to the magnetic properties of the light wave, this will influence the electron cloud density, causing it to shift towards the light wave (see figure 1.2B) [19]. This shift will be the strongest for a certain wave frequency, where this frequency of the wave matches with the plasmon frequency of the nanoparticle [22].

The plasmon frequency depends on many factors, such as the material, shape and size. Figure 1.3 shows

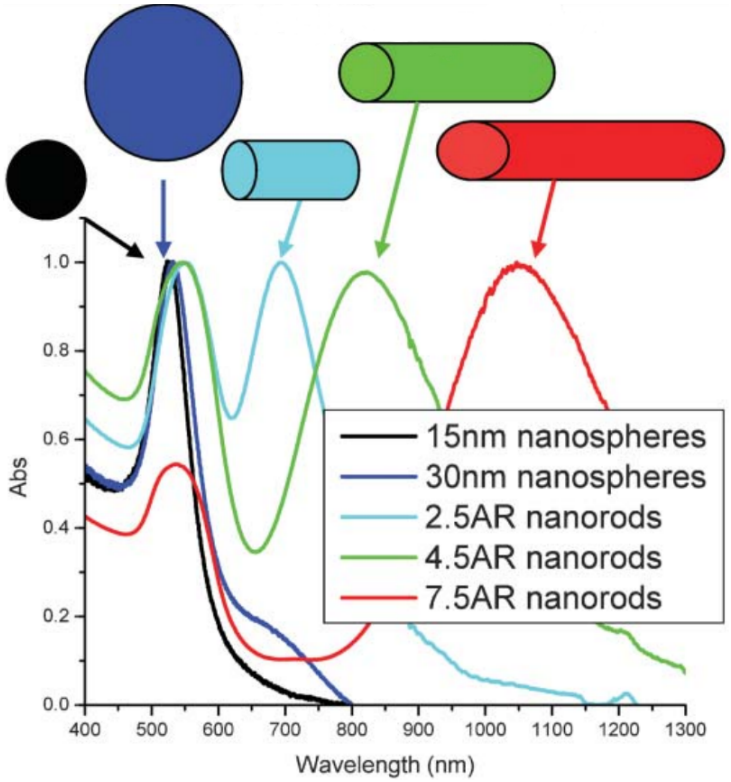

Figure 1.3: The absorption spectra for gold particles of different sizes and shapes. All the values are normalized. Source: [16]

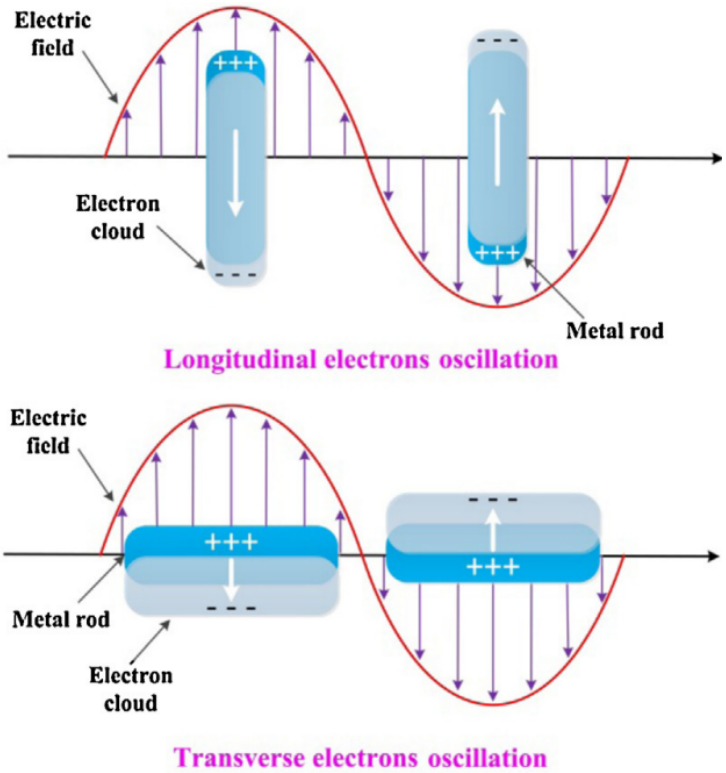

Figure 1.4: The two different plasmon peaks of rod shape particles, the longitudinal electron oscillation (or longitudinal surface plasmon resonance (LSPR)) and the transverse electron oscillation (or transverse surface plasmon resonance (LSPR)). Source: [23]

the differences between different sizes of gold nanospheres and nanorods. The bigger the gold sphere, the higher the plasmon resonances. This is because the bigger the particle, the more electrons shift, thus the less energy it costs to excite an electron. This is similar to the quantum mechanics model of *a particle in a box*, where, when the box gets bigger, it takes less energy to go to the next excited state. The higher wavelengths have a lower energy. Thus bigger particles result in red shifting; a bigger particle has a higher plasmon frequency wavelength. However, this red shifting effect doesn't have an large effect on the plasmon frequency as is visible in 1.3. Another thing that can be seen in figure 1.3 is that the rods have two peaks, while spheres only have one. The reason for this is the anisotropic shape of the rods. Figure 1.4 shows two kinds of plasmon resonances possible in nanorods; the one where the electron wave oscillates along the long axis of the rod and the so called longitudinal surface plasmon resonance (LSPR) and the one where the electron wave oscillates along the short axis of the rod, the so called transverse surface plasmon resonance (TSPR). The value of the TSPR will almost always be around the 520 nm. Bigger rods will have a slightly red-shifted TSPR. For LSPR the values can strongly vary. This difference depends on the aspect ratio (AR, length divided by the width). the LSPR doesn't depend on the exact dimensions of the rods, but rather the shape and thus the AR [14, 24]

Plasmon Enhanced Raman Spectroscopy

As mentioned before, the basis for electromagnetic enhancement has to do with this plasmonic effect. The surface plasmon resonance, which resulted from the interaction between a photon and the electrons at the surface of the colloidal particle, creates an enhanced local electromagnetic field surrounding that colloidal particle (see figure 1.2A). This field will enhance the localized electrical field (E_{loc} in equation 1.1) and thus the Raman spectroscopy intensity.

When two particles have a close interaction and at least one of them has a small radius or curvature - with small being somewhere in the order of nanometers - then the enhancement factor will be strongly increased (see figure 1.5) [23, 25, 26]. This happens when the plasmon resonance on the particles overlap in the near field [14]. These local enhancements are called 'hotspot' [27]. These hotspots can have an enhancement factor of 10^{11} depending on how strong the curvature is [28].

When molecules are close between the two plasmonic metals, the Raman process can be greatly enhanced due to these hotspot. This enhancement works in two steps. In the first step, the plasmonic metals work as a 'receiving optical antenna' enhancing the local field by focusing the optical beam to certain highly localised points. For the second step, the plasmonic metals are used as a 'transmitting optical antenna' where the Raman signal is transferred from the so called 'near field' to the 'far field' [22]. The overall enhancement depends therefore on the exciting field (which wavelength of the Raman laser) and emitting field (where is the plasmon resonance the biggest). Here the enhancement factor G_{SERS} can be seen as

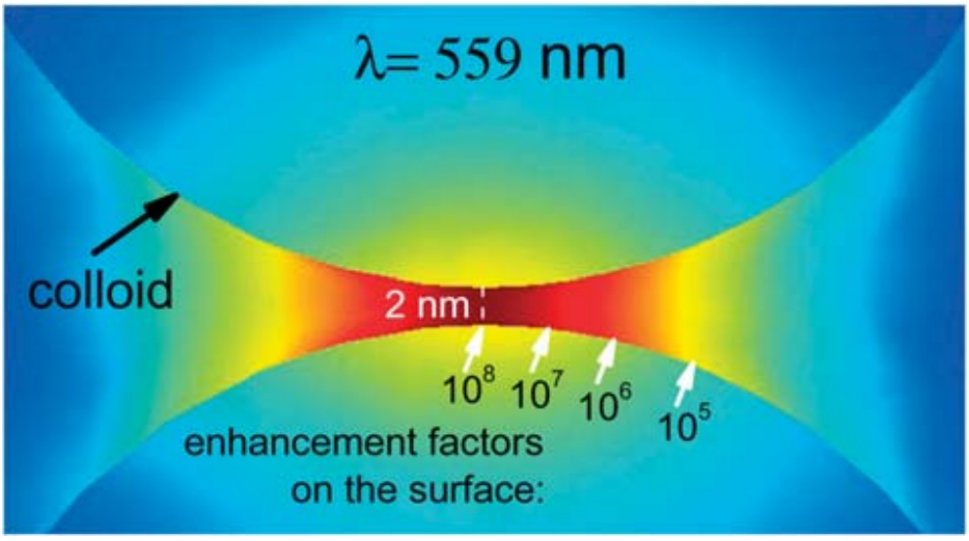

Figure 1.5: The SERS enhancement factors between two gold colloids with a radius of 30 nm with a polarization along the y-axis [25]

$$G_{SERS} \propto (\frac{E_{loc}(\lambda_{ex})}{E_0})^2 \cdot (\frac{E_{loc}(\lambda_{em})}{E_0})^2 = G_1^2 \cdot G_2^2 \tag{1.2}$$

With E_{loc} being the enhanced local electric field, at the exciting wavelength (λ_{ex}) or emitting wavelength (λ_{ex}), E_0 is the non-enhanced local field, G_1 being the enhancement factor for process 1 (receiving antenna) and G_2 being the enhancement factor for process 2 (transmitting antenna). Based on this equation it can be seen that if the wavelength of the plasmon peak and the Raman scattering signal are close to each other (thus G_1 and G_2 are similar) the enhancement is proportional to the fourth power of the enhancement of the local electric field. The strength of the local electric field of course depends on the distance between the metal surface and the molecule. It turns out this goes to the third power [22]:

$$E(r) \propto (1 + r/a)^{-3} \tag{1.3}$$

with r being the distance between the molecule and the metal surface, E(r) the local electric field and a the radius of the particle. Combining the last two equations shows that:

$$G_{SERS} \propto (1 + r/a)^{-12} \tag{1.4}$$

So it is really important that the molecule stays close to the metal surface [22]. There are a few strategies for doing this; the molecule can be anchored by creating a covalent bond between the ligands surrounding the metal and the molecule of interest, the antibody-antigen coupling is used and non-covalent bonding, such as van der Waals force or ionic bonds are used [22].

The use of the plasmonic effect to enhance Raman spectroscopy is called 'Plasmon Enhanced Raman Spectroscopy' [8]. This is a term that encompasses a few things such as Surface Enhanced Raman Spectroscopy (SERS) and Tip Enhanced Raman Spectroscopy (TERS). For SERS nanoparticles are used, which can be used in a colloidal fashion or grafted on a solid substrate. For TERS a large probe tip is used as a place for the enhancement [8]. SERS measurements can be done in a confocal Raman microscope, while for TERS a combination between a Raman microscope and a scanning probe microscope is needed. Also, since colloids are used for SERS, the target molecules can directly absorb on the substrate surface, which results in stronger enhancements. Further, for SERS particles with multiple hotspots can be used, allowing for more places with a strong enhancement, while for TERS there is only one hotspot, the tip. Thus the enhancement for TERS is lower than for SERS. [8] As SERS gives the highest enhancements, we will further investigate how these high enhancements can be achieved.

1.3 The ideal nanoparticle for SERS

For the use of SERS, a whole lot of different substrates are used [8, 27]. These substrates will differ in material, shape and structure. There isn't an unambiguously awnser to the question "which nanoparticle is the best for SERS". Many literature reviews have been written discussing that question [27]. However, here we will try to give an insight into the difference in materials and in shape and to give a conclusion on which particle would be the best for our purposes.

The material of the particle

A wide range of materials can be used for SERS. The most common metals are copper, silver and gold as these have an LSPR in the range of visible light or the near-infrared. However other metals can be used for other ranges, such as aluminium, which can be used for the UV range [30]. Even though not every metal is used, every metal is able, in theory, to give a plasmonic response. However, there is a big difference between the metals. Which metal makes a good plasmonic metal and why, is a complicated story, which mostly depends on the dielectric function of the metal. This is explained in great detail in various literature reviews such as by Blader et al in 2010 [29]. Figure 1.6, which originates from the same paper, shows the quality factor for the localised surface plasmon (QLSP) for all the non-f-block metals. Detail about how this precise quality factor is calculated is explained in the paper. It can be seen

from figure 1.6 that the alkali metals, the d11-metals and aluminium are good plasmonic metals. These metals all have 1 electron in their outer shell (S-shell for the alkali metals and d11-metals and P-shell for aluminium). This one electron gives a good dielectric response to greatly enhance the LSPR [29].

Of course, not only how strong the LSPR will be enhanced by the metal is important, but also the stability of the nanoparticles. It is well known that the alkali metals oxidize easily. This makes it hard to create nanoparticles out of these (and possibly also a bit dangerous). Gold and silver are pretty noble metals and thus hard to oxidize, making them quite stable. This, mixed with the great plasmonic response, makes them the most used plasmonic metals. Gold is probably used more than silver (even though silver has a stronger plasmonic response), as gold is more versatile [30, 31]. The reason begin that gold is more noble than silver and thus more chemical stable and there are an wider variety of nanoparticle shapes available for gold than for silver [30].

The shape of the particle

Not only the material of the nanoparticle is important for SERS, but also the shape of the particle. As mentioned before, the curvature of metallic particles used influences the enhancement factor. Because of this, for particles with an anisotropic shape, the enhancement isn't homogeneous surrounding the whole particle; at some places the enhancement is stronger and at other places weaker (see figure 1.7) [27].

Not only does the precise shape matter, but also the configuration of the nanoparticles. When nanorods are linked in an end-to-end configuration, the enhancement factor (EF) of these rods will be high, while for side-to-side the enhancement factor will be low and sometimes even lower than non-coupled particles [32–34].

So which particle shape then gives the best enhancement? A lot of papers and literature reviews have been published discussing all different kinds of (complicated) shapes and (assembled) structures and how good their enhancement factors are, aiming to answer that question [27]. However, using a complex shape might not always be better than using a simple one.

An example of this is the paper from Solis et al from 2017 [31]. Here they used electromagnetic computation techniques to calculate the enhancement factor for different kinds of gold nanoparticles (spheres, rods and stars) for different kinds of configurations. Some of their results are shown in figures 1.7 and 1.8.

Let's dive a bit deeper into these results. First, looking at individual particles in figure 1.7 (a, b, c), it shows that for spheres the enhancement effect of the electromagnetic field is even surrounding the whole particle. This is as expected since the whole curvature is even. Also, the enhancement is extremely low. (Notice the 1000x, meaning that they multiplied the data by this factor to get the colour for this enhancement. Even then, the colour is still at the low end of the scale). For the star-shaped particle, the

Li	Be		Element									B	C	Max Qlsp Key	
0.14*	0.20													0.00-2.99	
28.82	3.58		Frequency of Max QLSP		* Frequency is at the limit of the available data									3.00-3.99	
Na	Mg				# Low frequency data not included							Al	Si	4.00-5.99	
1.44	4.00		Maximum QLSP									11.00		6.00-9.99	
35.09	9.94											13.58		10+	
K	Ca	Sc	Ti	V	Cr	Mn	Fe	Co	Ni	Cu	Zn	Ga	Ge	As	Se
1.05	0.65*	0.3*	0.20	0.36	0.30	0.07*	0.10*	0.10*	0.15	1.75	3.60#	8.30			
40.68	3.63	1.02	2.58	4.27	2.16	1.16	2.48	2.69	2.71	10.09	3.59	3.41			
Rb	Sr	Y	Zr	Nb	Mo	Tc	Ru	Rh	Pd	Ag	Cd	In	Sn	Sb	Te
0.81	0.36*	1.48*	3.00	0.55	0.38		0.10*	0.30	0.10*	1.14	0.65#	5.10	2.25	3.50	
21.90	2.85	1.41	1.16	3.39	5.38		2.03	2.10	6.52	97.43	3.63	4.60	3.50	1.33	
Cs	Ba	Lan	Hf	Ta	W	Re	Os	Ir	Pt	Au	Hg	Tl	Pb	Bi	Po
0.51*	1.91		0.52*	0.58	0.30	0.10*	0.10*	0.40	0.35	1.40	4.20	3.20	5.95	3.50	
11.20	0.91		0.79	5.25	4.96	4.99	6.12	2.55	1.96	33.99	2.20	2.71	3.07	1.15	

Figure 1.6: A figure from [29]. In this literature review, they define a quality factor for the localised surface plasmon (QLSP). This figure shows how high this quality factor is for each non-f-block metal and they show the frequency at which this QLSP happens. More details are explained in the paper.

tips are enhanced strongly, due to the steep curvature. Rods have a stronger curvature at their tips than spheres, but not as strong as the tips of the stars. Their enhancement factors reflect this.

Looking at the dimers of the particles (figure 1.7, d, e, f), the strong effect of the coupling can be seen. For spheres, the enhancement is much more localized but stronger than before (notice the 10x). For rods this coupling effect is even stronger. For the stars, however, it doesn't seem to be a coupling effect. This is because these star shapes assemble in a "valley-to-tip" configuration. As the hotspot are only at the tips, a "valley-to-tip" configuration doesn't result in the hotspot being close to each other. Because of this, no increase in the strength of the SERS can be seen when the particles come close to each other. It is even worse as increasing the concentration of gold star particles could dampen the incoming light and thus decreases the enhancement [31].

Figure 1.8 shows how the SERS enhancement will differ when more and more particles are added to the monolayer (called coverage in the plot, meaning which percentage of the monolayer is gold and not empty space). It can be seen that for both the gold nanoparticles and nanorods the intensity increases when the coverage increase, especially after a certain threshold. For the gold nanostars, this increase isn't present. This figure also shows that when the gold particles are enhanced at a wavelength of 785 nm the enhancement of the gold nanorods surpassed the enhancement of the nanostars and goes to almost the same height as the enhancement of the gold nanostars at their optimum wavelength (900 nm). This further proves that the particle with the most edges and curves isn't necessarily the best particle to use to optimize SERS.

In this thesis, we chose to use rods. They give a better enhancement than spheres and similar (and maybe even better) enhancements as more complex shapes. Also, the synthesis for rods is relatively easy compared to more complex structures. Further, it is easier for rods to change the synthesis to gain particles where the peak of the plasmonic response is at a different wavelength than with more complex shapes. Another reason to use rods is that their self-assembly is well known and we can use that to further enhance the SERS.

1.4 Self-assembly of rod-like particles

Liquid Crystal Structures

Self-assembly is the term used for the way (colloidal) particles and other macrostructures order themself due to the influence of thermodynamics [36]. A famous example of this is the formation of micelle structures by soap-like molecules, which happens due to electrostatic interactions of the polar and apolar

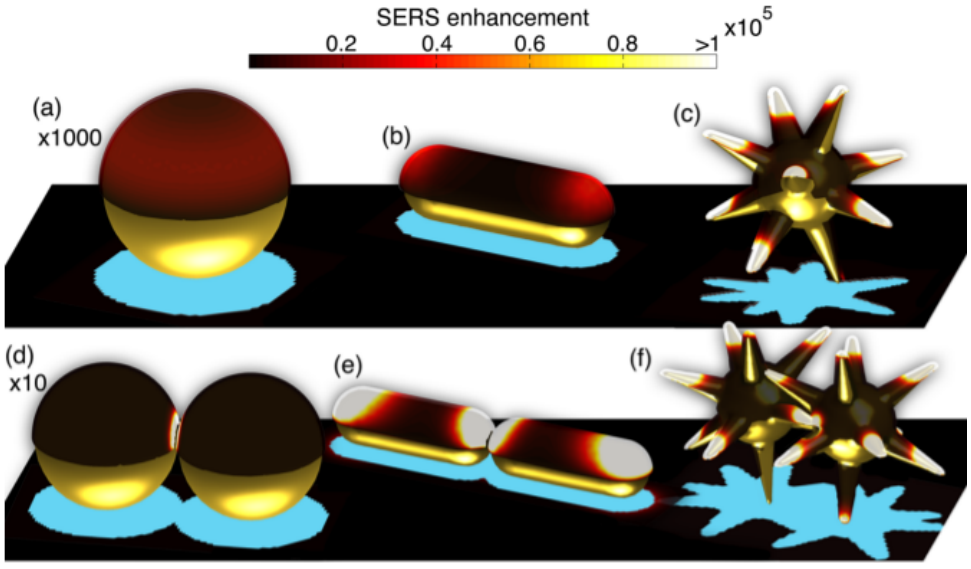

Figure 1.7: The near-field analysis of the SERS enhancement for three different gold nanoparticles (spheres, rods and stars), showing both the enhancement factors for individual particles and when coupled as a dimer. The data for the spheres (a and d) are multiplied by a factor 1000x and 10x respectively. Source [31]

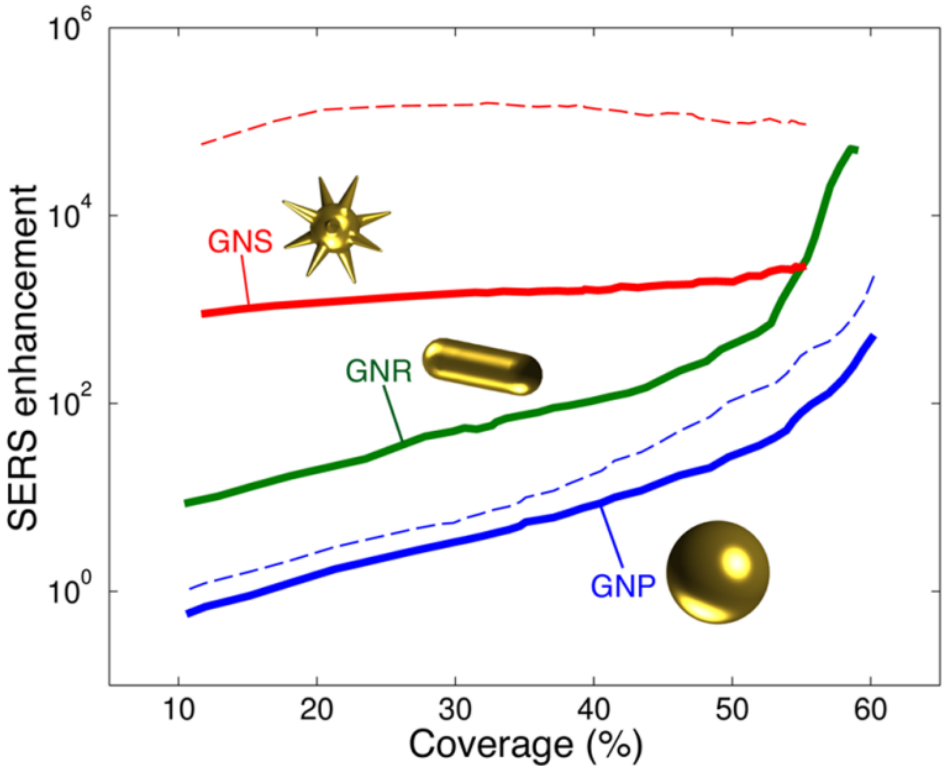

Figure 1.8: The average calculated SERS enhancement for different gold nanoparticles under different percentages of coverage for a planar monolayer. The solid curve corresponds to an incident wavelength of 785 nm, which is according to the paper the most common Raman laser, and the dashed line corresponds to 633 and 900 nm for the gold nanoparticle (GNP) and gold nanostars (GNS) respectively. These wavelengths are the optimum wavelengths for these particles. Source: [31]

parts of the molecules. These interactions drive the polar parts to each other and the apolar parts,

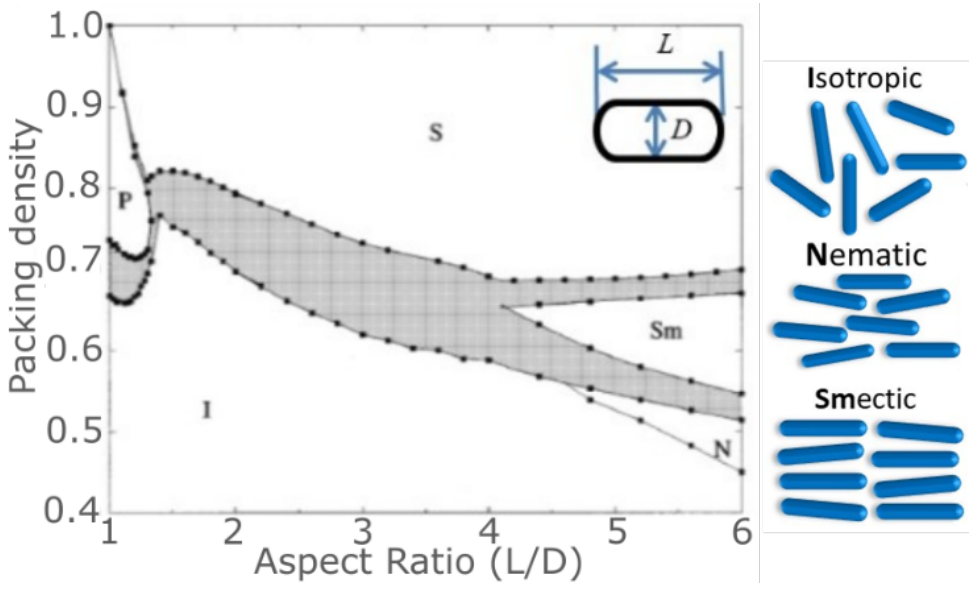

Figure 1.9: On the left, the phase diagram of hard-core spherocylinders with different aspect ratios and packing fractions based on computer simulation. On the right the three different liquid phases for rods. The thick letters correspond with the letters used in the diagram. S and P in the diagram stand for solid and plastic phase. Source: [35]

creating a micelle structure.

Hard rod shape particles (such as gold nanorods) can also self-assemble. Hard sphere particles arrange in different liquid crystals if the packing density is high enough. For rod-shaped particles three different liquid crystal phases are known, depending on the aspect ratio of the rods and their packing density [35]. Figure 1.9 shows how changing the aspect ratio and packing fraction of the rods results in different phases. It shows that if the packing order is low enough an isotropic order will be formed, even at high aspect ratios. At aspect ratio 4.1 and 4.7 smectic and nematic ordering can be formed respectively if the packing fraction is high enough.

As discussed in chapter 1.3, the SERS enhancement factor for rods is the strongest in an end-to-end configuration [34]. Using the smectic ordering of rods would be a novel way of creating end-to-end configuration without the need for further synthesis steps (such as the creation of linker polymers between the gold rods).

To create a good smectic ordered system, it is important not to have too much polydispersity. The more variation there is between the particles, the less energy gain there is for forming this smectic ordering. Based on Monte Carlo simulations, it has been shown that when the polydispersity of the nanorods is above 8%, then smectic ordering can become unstable where above 18% the smectic ordering disappears completely [37].

Van der Waals interactions

An important parameter to consider for the self-assembly is the van der Waals interaction. Gold is known to have a high van der Waals interaction [38]. Further, the van der Waals potential is linked to the volume of an object. If the van der Waals potential becomes too high, then this can influence the self-assembly as the particle will stick and aggregate and not form a nicely smectic ordered structure. A 'simple' way to prevent aggregating is to form a physical barrier surrounding the gold rod, preventing two particles from coming too close and thus aggregating. In this thesis silica is used as the physical barrier. Further, the use of silica also increases the thermal stability, increases solubility in apolar solvents and could be used as a template for further synthesis on the gold rod [39]. More on silica will be explained in chapter 3.

It is important to get an estimation of how thick this physical barrier should be. The thicker the physical barrier, the lower the aspect ratio of the rod will become. However, if the physical barrier is too thin, then the particles could aggregate. To get an idea of how thick this physical barrier should be, the van der Waals interaction of two (identical) rods can be calculated. This can be done in the following way [40]:

$$U_{vdW}(z) = -\frac{3}{8\pi} A_H \frac{(\pi R^2)^2 L}{z^5} \tag{1.5}$$

This formula calculates the side to side van der Waals interactions of two identical rod shape particles.

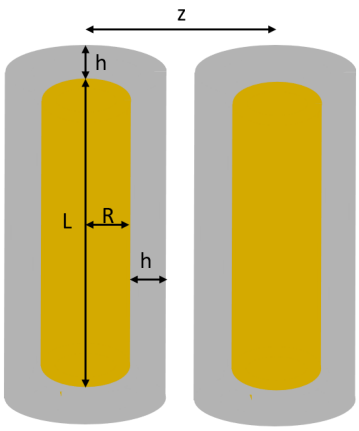

Figure 1.10: An schematic of two silica coated gold nanorods, showing the gold rod in gold and the silica layer in grey. The letters added correspond to the physical quantities in equations 1.5 and 1.6.

Here the van der Waals interaction is the strongest, as it gives the most surface contact. In this formula is $U_{vdW}(z)$ the van der Waals interaction at a distance z, with z being the distance between two rods (core to core), L is the length of the rod and R is the radius of the rod. See also figure 1.10. A_H is the Hamaker constant, which tells something about how strong the van der Waals interactions are for a certain material in a certain medium. For colloidal gold in water, this value is between $8.22 \cdot 10^{-20}$ J and $3.00 \cdot 10^{-19}$ J (or 20 and 73 k_bT at room temperature). For silica in water the Hamaker constant is around $3\text{-}4 \cdot 10^{-20}$ J or just below 1 k_bT [41]. Since the van der Waals attraction of the gold is around 20 to 75 times bigger, the van der Waals attraction of the silica can be ignored, which makes the calculations easier.

To estimate the thickness of the silica layer, the van der Waals potential between two coated gold rods parallel to each other (where the van der Waals potential is the highest) could be calculated. If the thickness of the silica layer is defined as 'h' then the closest two particles can come is 2R+2h (note that the van der Waals potential is calculated from the centre of mass, hence the 2R). This would change equation 1.5 to:

$$U_{vdW}(2R+2h) = -\frac{3}{8\pi} A_H \frac{(\pi R^2)^2 L}{(2R+2h)^5} \tag{1.6}$$

To get some insight into the physical meaning of this equation, figure 1.11 is created, which shows U_{Vdw} as a function of h for different values of R. It shows how strong the van der Waals interaction would be if two gold nanorods of an arbitrary length (for the calculation L = 75 nm was chosen) with different radii if they were separated by a silica layer with variable thickness.

Figure 1.11 shows that the shorter the silica layer surrounding the particle is, the stronger the van der Waals interaction. Ideally, the silica layer would be as thick as possible, to keep the van der Waals interaction as low as possible. However, a thick silica layer increases the aspect ratio of the particle. So an optimum needs to be found between having a thick enough silica to prevent aggregation and thin enough particles to have a high enough aspect ratio to form smectic ordering.

Since a thinner silica layer will always lead to more van der Waals interaction, the question is: how much van der Waals interaction is too much? According to the equipartition theorem [42] the average kinetic energy of hard sphere is 1.5 K_BT.This value could be used as some sort of lower limit (lower, since the energy is negative) for the value that the van der Waals potential. The idea being that as long as the kinetic energy of the particle is higher than the van der Waals potential, the particle can still 'break loose' if it 'aggregated'. This is of course a bit of oversimplification, however, the whole calculation is only an approximation. This value is shown in figure 1.11 as the green line.

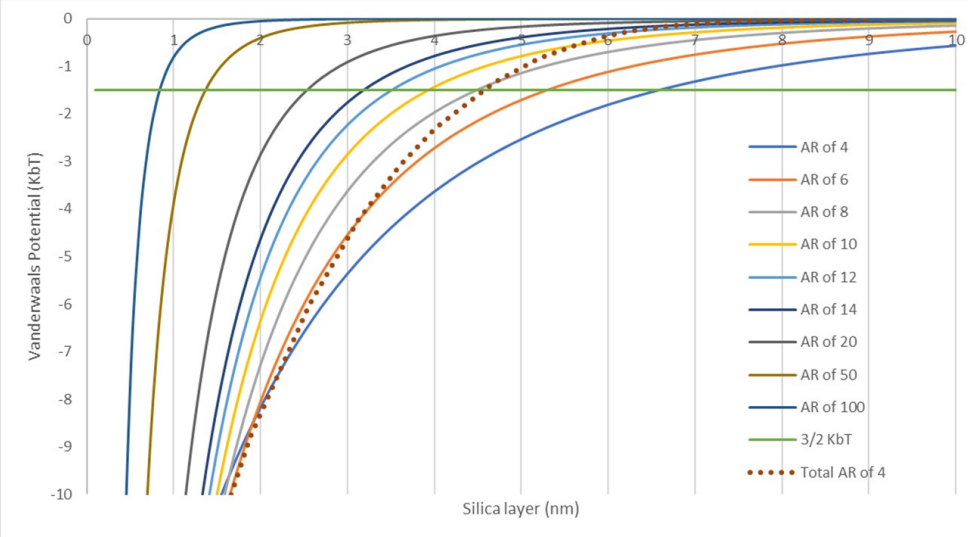

Figure 1.11: A calculation of the side to side van der Waals interaction between two gold nanorods is water for various silica layer thicknesses in between. the calculations for gold nanorods with different aspect ratios, AR, (from 4 to 100), based on the equation 1.6. L = 75 nm and A_H = 73 K_bT

Another way of looking at what the maximal value of the van der Waals potential is, is by assuming that the distribution of the particles is some sort of Boltzmann distribution. One can think of a two-state system. In one state (state 1) the particles are as close as possible (thus z=2R+2h) and in the other state (state 2) the particles don't interact with each other (thus are 'infinite' apart). The Boltzmann distribution can be approximated as:

$$P = \frac{1}{1 + exp\left(\frac{-\Delta E}{K_B T}\right)} = \frac{1}{1 + exp\left(\frac{E_2 - E_1}{K_B T}\right)} \tag{1.7}$$

were P is the chance a particle is 'aggregated' (thus in state 1), Δ the energy difference between the states, K_b is the Boltzmann constant and T is the temperature (here assumed as room temperature or 298K). E_1 can be defined as

$$E_1 = U_{vdW}(2R + 2h) = -\frac{3}{8\pi} A_H \frac{(\pi R^2)^2 L}{(2R + 2h)^5} \tag{1.8}$$

And E_2:

$$E_2 = U_{vdW}(\infty) = -\frac{3}{8\pi} A_H \frac{(\pi R^2)^2 L}{(\infty)^5} = 0 \tag{1.9}$$

Making equation 1.7 into

$$P = \frac{1}{1 + exp\left(\frac{-E_1}{K_B T}\right)} = \frac{1}{1 + exp\left(\frac{-U_{vdW}(2R+2h)}{K_B T}\right)} \tag{1.10}$$

For a value of 1.5 K_bT P becomes 0.82. This means that at any given moment 82% of the particle are in the 'aggregated' state. This may seem high, but remember, this is only a two-state system. So the particles are either completely attached or not at all. Also here we are only looking at one attraction and no repulsion. So 82% seems reasonable. The exact cut of value is actually completely arbitrary, but less than 90% in the 'aggregated' state feels good.

Based on this calculation we could conclude that the cutoff value should be around the value of the kinetic energy of the particle as mentioned before. If one would increase the cut-off value of the van der Waals interaction to 3 K_bT then less than 5% of the particles would be not aggregated, which is clearly too low. What this shows is that the maximal value of the van der Waals interaction maybe isn't 1.5 K_bT, but should be somewhere in that order of size. It is clear that 3 K_bT is already too high, which gives insight into how thick the silica layer should be at least.

Another thing to look into is how the thickness of the silica layer influences the aspect ratio of the nanorod. Since the aspect ratio should not be higher than 4.1, we could calculate how big the value of R can be for eavery 'h' and then use equation 1.6 to calculate the value of U_{Vdw} for these values of R and h. This is the brown dotted line in figure 1.11. The actual van der Waals potential values of this brown line don't really have a physical meaning, but the points where it cuts the other coloured lines show the maximum the silica layer can be before the whole particle will exceed the aspect ratio of 4.1.

Figure 1.11 is created by choosing an arbitrary rod size. However, it would be more useful to look at equation 1.6 in units of aspect ratio. To do so the equation needs to be rewritten. The aspect ratio for gold nanorods can be defined as follows:

$$\Gamma_G = \frac{L}{W} = \frac{L}{2R} \tag{1.11}$$

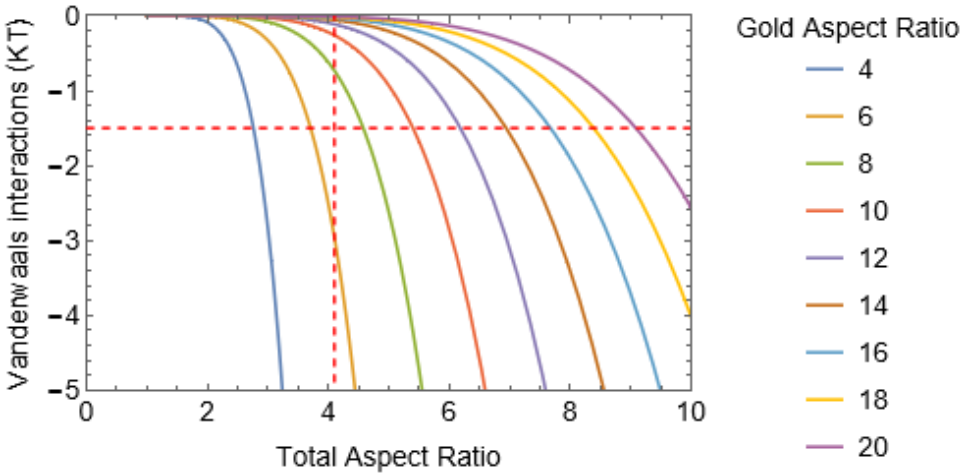

Figure 1.12: The van der Waals interaction of gold rods with different aspect ratios with various thicknesses of silica layer (total aspect ratio) based on equation 1.13.

were Γ_G is the aspect ratio of the gold rod (called *gold aspect ratio*), L is the length of the rod (from tip to tip), W is the width of the rod and R is the radius (which is half the value of W by definition).

And the aspect ratio for gold nanorod coated with a silica layer using (Γ_T, or *total aspect ratio*):

$$\Gamma_T = \frac{L + 2h}{2R + 2h} \tag{1.12}$$

where h is the thickness of the silica layer. As the gold rod is coated with silica at both sides of the rods, both the length and the width of the gold rod are coated by two times the thickness of the silica layer. Using these definitions equation 1.6 can be rewritten to (see also appendix):

$$U_{vdW}(z) = -\frac{3}{128}\pi A_H \frac{\Gamma_G(1-\Gamma_T)^5}{(1-\Gamma_G)^5} \tag{1.13}$$

Equation 1.13 shows that the van der Waals interaction between the two coated rods does not depend on solely the length of the width of the particle, but can completely be rewritten to be dependent on the aspect ratios. This shows that there is not an ideal length or width for the nanorods (for the van der Waals potential) and thus that the length and width of nanorods solely depend on practical means. In figure 1.12, this equation is plotted for different gold aspect ratios.

Figure 1.12 shows similar information as figure 1.11, but now in terms of aspect ratios. The two red dashed lines show the average kinetic energy (1.5 K_BT, negative to use as a comparison) and the total aspect ratio of 4.1. To get a good estimation of what the minimal aspect ratio of the gold rods should be, it can be calculated which value (Γ_G) should have to go through the crossing of these lines. This is calculated to be 6.9 (see appendix). This means that if the gold rod has an aspect ratio lower than this, then the silica layer needs to be so thin for an aspect ratio of 4.1 that it is no longer thick enough to prevent aggregation.

On the previous page, we shortly touch on what the value of the van der Waals interaction should be. Here 1.5 K_BT was chosen, which was a sort of arbitrary value. Since the value of the van der Waals interaction is reasonable between 0.7 and 3.0 K_BT, the values of Γ_G for these values are 8.1 and 6.0 respectively. Note that these values are all calculated for a total aspect ratio of 4.1, which is the absolute minimum the rods should have to form the smectic ordering. However, it is better to go for a slightly higher aspect ratio, say 4.5. Here there is more room to obtain the right packing density. Also, since the silica particles have a slight charge, it could well be that this charge influences the self-assembly a little bit. To neglect this effect, the rods can be assumed of being slightly bigger than they really are. This also makes going for a slightly higher aspect ratio would be better. If we aim for an aspect ratio of 4.5 then the gold rod aspect ratio would already increase to 7.5 (for 1.5 K_BT, for 0.7 and 3.0 K_BT the gold

aspect ratios would become 9.2 and 6.8 respectively.). This shows that if one would try to make gold rods for the purpose of coating them in silica and forming smectic ordering, then one should try to make rods with an aspect ratio of at least 7.5, but something high like 9 or 10 would be better.

A few remarks about these calculations. These calculations should be seen as an estimate of the parameters needed. This calculation is only based on the van der Waals attraction using only the side-to-side attraction. To get a more precise estimate of how low the aspect ratio of the gold rods could be, one could calculate way more different interactions (end-to-end attraction of van der Waals or the static repulsion of the silica layers etc.). But since the van der Waals attraction of the end-to-end configuration should be less than the side-to-side configuration and the static repulsion would be counteracting the van der Waals potential, only calculation of the side-to-side potential should give an a decent estimation.

1.5 Aim and outline

The aim of this thesis is to create smectic-ordered silica-coated gold nanorods. As discussed before gold nanorods will maximize the SERS enhancement. The smectic ordering should further increase the enhancement due to the end-to-end coupling. The silica layer will prevent the rods from coming too close and damping the signal and aggregated.

This thesis is structured the following way: Chapters 2 and 3 are dedicated to the synthesis of gold nanorods and the coating of the gold nanorods in silica respectively. Each chapter will start off with a little bit of theory explaining how the synthesis works and why we do them. Since the results of one synthesis will influence the steps taken for the next synthesis, there will not be a whole section explaining all the different synthesis steps and then discussing all of the results, but this will be done much more on a per-experiment basis, to ease the story and prevent constant back and forward referring and thus improve overall readability.

This thesis will end with Chapter 5, which will give an overview of the most important results and give an overall conclusion and an outlook for the project.

2 Gold Nanorods

2.1 Theory of gold nanorod formation

Synthesizing gold nanoparticles

Gold can be used to make many nanostructures; spheres [43], rods [17, 44], cubes [45], triangles [46] and even stars [47]. All these particles can be made via a so called bottom-up approach where the particles are created from gold ions. This is done via the so called wet-chemical method [48]. Which particle shape is formed exactly is an interesting interplay between thermodynamics and kinetics, where the use of the right surfactants and experimental parameters dictate the end shape. The formation of gold nanoparticles goes in three steps. First small clusters of a few atoms are formed. Then these clusters grow into seeds with a well-defined structure. Last these seeds are then used as a base for the growth of the actual nanoparticle [49]. Usually, the formation of seeds and actual particles are done separately (seeded growth) [17, 44, 49]. However, it is possible to create gold nanoparticles where all three steps happen in the same environment (so called one-pot synthesis) [50]

In general, the shape of the nanoparticle via the seed-mediated method is influenced by the surfactants used (see figure 2.1). These surfactants influence the growth kinetics of certain facets of the gold nanoparticle. This results in certain facets growing faster and others growing slower. The interplay of the kinetics between certain facets, surfactants and gold ions is what eventually results in the end shape of the particle as shown in figure 2.1. One could think that using no surfactant would result in spherical particles as all the sides would grow at the same speed. This, however, isn't the case. As gold atoms want to be next to each other to form a solid grid, but they also want to limit the surface tension. The end result is a hexal or octahedral structure. Hard corners (such as with a cube) are not ideal as they have a lot of surface tension, so they are limited. These two things (limiting the surface tension and atoms wanting to have as many neighbours as possible) result in this octahedral structure. This octahedral structure has a few different facets, which will have different kinetics due to different surfactants and reactants. By using this difference in kinetics, one can influence the shape of the particle as is shown in figure 2.1 [51].

Since kinetics play a large role in the formation of these gold particles, they are highly susceptible to small changes in the protocol, such as stirring speed or temperature. For example, a change of one degree K can change the aspect ratio of a gold nanorod by 0.2 [52]. This seems small, but it is significant when trying to achieve monodisperse particles. Also, something small as impurities of the surfactants can have a big influence on the end product. It has been shown that changing the supplier of the commonly used surfactant CTAB (cetyltrimethylammonium bromide) can result in the success or failure of the synthesis. This has to do with trace amounts of iodide, which influences the reduction of gold(III) to gold(0) and can be adsorbed on the 111-surface of the gold particle inhibiting the nanorod growth, resulting in the formation of gold nanospheres instead of the wanted nanorods [53].

Synthesizing gold nanorods

As mentioned in the introduction, the desired shape for the gold nanoparticle for this thesis is the rod shape. For this thesis, two methods, as reported by Ye & Murray [44] and Chang & Murphy [17], were

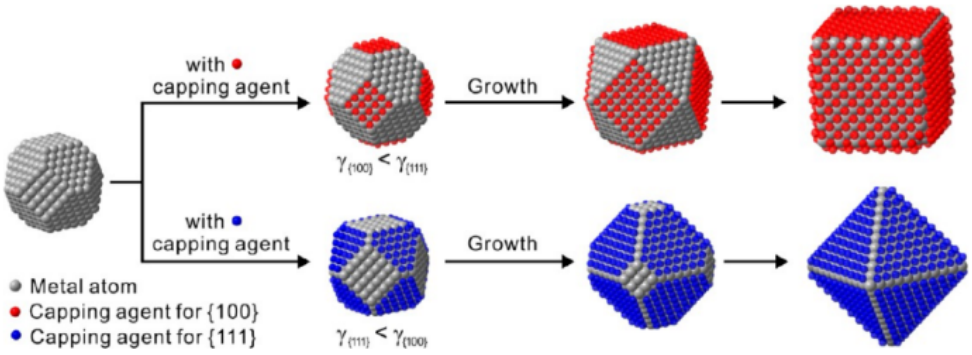

Figure 2.1: A diagram showing how the use of a different capping agent can change the shape. The red capping agents will make the 100-facets grow faster, while the blue capping agents will make the 111-factes grow faster, resulting in distinct shapes. Source: [51]

used to synthesise Au NRs.

Both these methods use the seed-mediated growth method. The seeded-mediated growth leads to a higher yield and fewer shape impurities. This is because the conditions needed to form the seeds differ strongly from the conditions needed to create rod shape particles; to form the seeds a strong reducing agent is needed, which reduces the Au(III) atoms of the $HAuCl_4$ complex directly to Au(0). These Au(0) atoms cluster together to slowly form the seeds. This is done in more extreme (acidic) conditions than in the growth solution, as the Au(0) atoms need to cluster together. Due to the electron configuration, Au(0) atoms by themselves aren't stable and are way more likely to oxidize to Au(I)[1]. A cluster of Au(0) atoms is stable. In the extreme (acid) conditions of the seed solution, a few Au(0) exist long enough to cluster together creating a stable particle. Over the ageing process in the seed solution, these clusters grow to form small seeds of around 3.5 nm [54]. Because the seeds will be added to the growth solution after they are fully formed, all the rods will start growing from the same starting position (namely, the 3.5 nm seed). This limits polydispersity compared to the seedless method, were seeds can form at any time [49].

The general synthesis of the gold nanorod formation is based on the following half-reaction:

$$3Au^{+} \leftrightarrows 2Au^{0} + Au^{3+}$$

Since Au(0) atoms on their own aren't stable, due to the electron configuration, new Au(0) can only form directly next to existing Au(0) atoms [49]. In the growth solution, a soft reducing agent is used. The soft reducing agent reduces the Au(III) of the $HAuCl_4$ complex to Au(I), but not to Au(0). Because of this, a lot of Au(I) ions are present in the growth solution. These will react with the seeds to form new Au(O), directly next to existing Au(O) atoms (and thus growing the particle, without the formation of new seeds), and Au(III). Due to the soft reducing agent still present in the solution, the newly formed Au(III) atoms will oxidize back to Au(I) which can react again. This reaction will repeat until all the Au(I) has reacted and no Au(III) is formed or when all of the reducing agent has reacted.

When a one-pot synthesis is used, then a strong acid is needed, which will form the seeds. But these seeds will already start to grow, while still new seeds are formed. Because of this, there are a lot of different components present at the same time. At a given time there are going to be seeds which are just formed, seeds that are already fully formed an in the proces of become in a rod, rods that are growing and fully formed rods. Because solvent should in theory accomidate for all these species, this will increase polydisperity and the amount of shape impurities compared to the seeded method. The use of a seed-mediated growth allows for two solutions, one where small seeds can form with the use of strong acids and then all these seeds can be added to the growth solution at the same time, allowing for all the particles to grow simultaneously. Also, a soft acid can be used in the growth solution to prevent new seeds from forming. Because of this, the seed-mediated method has a lower degree of polydispersity and fewer shape impurities.

To make sure that rods are formed and not spheres, a symmetry-breaking step is needed. As mentioned before, the surfactants play here a large role. CTAB is widely used [49]. The long carbon tail and charge head group (quaternary ammonium) of the CTAB molecules makes it a soap-like molecule which forms rod shape micelles. It was thought that these rod-shaped micelles help in the formation of rod shape particles, but recent studies show that this hypothesis is false [55]. However, CTAB can act as a face-specific capping agent. It binds preferentially to the longitudinal faces, slowing down the growth at those faces, resulting in longer gold nanoparticles (a.k.a rods) [56].

Another important chemical for the symmetry-breaking step is $AgNO_3$. The presence of Ag^{+} around the gold surface stabilizes the 011-type surface [55]. These factes are generated when the seeds start to grow in the longitudinal direction due to CTAB. The ratio between the concentrations of $HAuCl_4$ and $AgNO_4$ affects at which point the symmetry-breaking steps happen in the growth process and how fast the rods grow (especially in the length). This is until at a point too much silver is added and the silver ions and chloride ions start aggregation with each other and no rods are formed at all [55]. For this effect, the pH of the solution is also strongly influential. Because of this, some HCl is also added to the growth solution [49]. Both the ratio between silver ions and seed solution as well as the pH can be used to control the aspect ratio of the gold rods [17, 44].

[1] The electron configuration of Au(0) is [Xe]4f14 5d10 6s1. For Au(I) is [Xe]4f14 5d10. Thus Au(0) has one electron in its outer s shell, while the d shell is completely filled. For Au(I) this s shell is empty while it still has a completely full d shell. One could say that the elemental gold Au has one electron too many. For this reason, platina, the element left of gold in periodic table, is more stable than gold. Likewise, single atoms of Au(I) are more stable than single atoms of Au(0) [49]

The role of the chemicals used in the gold nanorod synthesis

Let's dive a bit deeper into the synthesis mechanism and look at the role of the different chemicals used. Here only the role of these chemicals will be discussed. The precise protocol of the two syntheses will be discussed later.

In both the seed solution and growth solution cetyltrimethylammonium bromide (CTAB) is added along with the $HAuCl_4$ complex and both are dissolved in water. As discussed CTAB is important for rod shape in the end. However, CTAB does have a few extra influences. First, CTAB can stabilize gold particles, making them soluble in water and preventing aggregation [49]. Second, the halide inside the CTAB molecule is crucial for the creation of rods [56]. The Br-ions will swap with the chloride ions of the gold complex to form $HAuBr_4$[2]. changing the redox potential [49]. It is crucial to use bromide; using CTAC (cetyltrimethylammonium chloride, the same molecule except with a chloride instead of a bromide) results in a failed synthesis and spherical particles. Even a 1:2 ratio CTAC:CTAB leads to a failed synthesis [57]. Due to the swapping of the ligand surrounding the gold atoms (from chloride to bromide), the colour of the solution will change from pale yellow to a more orange-yellow colour. It is important that all the gold atoms are dissolved and the ligand exchange was successful. Further, when the CTAB and $HAuCl_4$ are added together, some small clumps are observed in the solution. The quaternary ammonium group inside at the head of the CTAB molecule can form a neutral complex with the $HAuBr_4$. This complex is insoluble in water. The small clumps in the solution are this neutral complex. To make sure all the gold atoms are dissolved, the ligand exchanges are fully finished and no more clumps are present, it is good practice to stir the mixture of $HAuCl_4$ and CTAB for at least 10 min before continuing with the synthesis [49].

After the CTAB and $HAuCl_4$ are properly mixed in the seed solution, a strong reducing agent is added to form the seeds. This reducing agent should be strong enough to completely reduce the Au(III) to Au(O). $NaBH_4$ is used in almost every synthesis. [49]. As soon as the $NaBH_4$ is added to the seed solution a strong colour shift will happen. The solution becomes almost colourless with a light yellow brownish colour. This collor shift happens because the Au(III), which is yellow, is reduced to Au(I) and then Au(O), which both are collorless [49]). The brown color is due to small seeds already formed. After ageing for a few minutes, the solution becomes more brown as the last of the AU(III) reacts (and thus the solution looses its yellow color) and the seeds become bigger (and thus the solution becomes more brown) [49]).

After ageing for a few minutes, the solution becomes more brown as the seeds begin to grow towards their final shape. The whole solution becomes colourless due to all the Au(III) being reduced to Au(I) and then Au(O) (both are colourless [49]). Even though the seeds are small gold nanoparticles, the color of the solution doesn't look like the plasmonic colours. That is because the 3.5 nm of the rods is to small for the plasmonic effect to take place [55]. The brown colour of the solution is the interband emission of the Au(0), which reminds of the colour of bulk gold, without the shining property [49].

As $NaBH_4$ is hygroscopic and thus can react with the water in the air, it is important to prepare the $NaBH_4$ solution as fresh as possible (not older than 1 minute) [44]. Further, the $NaBH_4$ will react completely within seconds when put in the seed solution. Because of this, it is good practice to stir the solution as strongly as possible and the $NaBH_4$ needs to be added straight in the middle of the flask. This will improve the homogeneously of the distribution in the few seconds the $NaBH_4$ reacts with its environment. This will improve the homogeneously of the seeds, which will lead to more homogeneous rods [49]. To slow down the reaction of $NaBH_4$ with water, a more basic solution can be created by dissolving some NaOH. $NaBH_4$ reacts with H^+ to form H_2. By increasing the pH, less H^+ is present and thus the reaction speed of $NaBH_4$ goes down. Another way of slowing down the reaction speed of $NaBH_4$ is using cold water, as this will lower the thermal energy of the system. In these syntheses, both these things are used. Still, the most important thing is to limit the time between $NaBH_4$ solution is prepared and the solution is added to the seed solution [49].

To prepare the growth solution a mixture of CTAB and $HAuCl_4$ is prepared, similar to the seed solution. In one of the two syntheses, sodium oleate (NaOL) is also used [44]. The double bond in the tail of the NaOL molecule is able to slowly reduce the Au(III) to Au(I). Also, the NaOL will form with CTAB a binary mixture which will influence the dimensions of gold nanorods, as the NaOL will work as a capping agent together with the CTAB. The addition of NaOL to the growth solution turns this solution colourless over time. This is because of the reduction of gold atoms from Au(III) to Ah(I).

[2] according to ligand Field Theory, bromide is a stronger ligand than chloride [56]

For the formation of gold nanorods, a lot of chemicals are used. Making gold nanorods isn't an easy synthesis. There are a lot of steps and small changes can have big influences. Such as a small change in temperature [52] or changes in the chemical supplier as mentioned earlier [53]. However, by working precisely, it is doable to create nice gold nanorods.

2.2 Synthesis of Gold Nanorods via the Ye & Murray's method

The synthesis most commonly used in the SCM group to make gold nanorods is a method reported by Ye & Murray et al. This method gives high control over the size and aspect ratio and yields highly monodisperse Au NRs for most sizes. The nanorods obtained are mono-crystalline with little to no shape impurities.

Synthesis

Preparing the seed solution: 10.0 mL 100 mM CTAB in a 40 mL vial was placed in a 30 °C water bath while stirring at 400 rpm. 51.0 µL 50.0 mM $HAuCl_4$ was added. A small colour shift from pale yellow to deep orange was observed as the ligands surrounding the gold atoms change from Cl^- to Br^-. Some solids were formed. The solution was left to stir for several minutes to make sure that the gold properly was dissolved. A 100 mM $NaBH_4$ solution was prepared by quickly weighing $NaBH_4$ and immediately dissolving it in cold (4.0 °C) water. Then immediately diluted it to 6.0 mM $NaBH_4$ using ice-cold DI water. Within 30 seconds, 1.00 mL was added to the seed solution, while stirring at 1200 rpm. After two minutes the stirring was stopped and the seeds were aged for at least 30 min.

Preparing the growth solution: A water bath of 50 °C was prepared. In a 500 mL Erlenmeyer flask a mixture of 7.00 g CTAB and 1.25 g NaOL were prepared in 250 mL deionized water (in the rest just referred to as 'water') were added. The mixture was placed in the water bath and stirred at 500 rpm until the compounds were dissolved (in about 30 min). The mixture was cooled to 30 °C by changing the water in the water bath. Then 4.80 mL 10.0 mM $AgNO_3$ was added to the growth solution and stirred for 30 seconds. Later, stirring at 400 rpm, a 250 mL 500 µM $HAuCl_4$ solution (prepared by dissolving 5.00 mL of the 50.0 mM stock solution $HAuCl_4$ in 245 mL water) was added and the mixture was left for 90 min while stirring at 400 rpm. The growth mixture quickly turned to an orange colour and then slowly colourless. The seed solution was prepared in the meantime. After 90 min 2.10 mL HCl (37% solution in water) was added while stirring at 500 rpm. After 15 min, 1.25 mL 64.0 µM AA and 800 µL seed solution was added while stirring. After 2 min of stirring, the growth mixtures were left unstirred at 30 °C overnight.

Washing: After the growth mixture has aged overnight (around 16 hours), a red-brown colour was observed. The 500 mL growth solution was divided over twelve falcon tubes of 45.0 mL. After the tubes were balanced by transferring the mixture from one tube to another and were centrifuged at 8000 rcf for 40 min at 23 °C. Then the supernatant was removed. The sediments were combined into four tubes. Each tube was dissolved in 40.0 mL water and centrifuged again with the same settings. After centrifugation, the supernatant was discarded and the sediment was redispersed in 35.0 mL 5.00 mM CTAB and stored in a 40.0 mL vial.

Changing the AR of the Ye & Murray's method: Described above is the general method to make gold nanorods of AR 3. The gold batches Au-NR001 until 006 were synthesized this way and all have an aspect ratio around this value (see table 1). Increasing the amount of $AgNO_3$ and HCl added to the growth solution higher AR rods are synthesized. One batch with a higher aspect ratio (5.5) was made, Au-NR007. Here 7.20 mL of 10.0 mM $AgNO_3$ and 3.00 mL HCl (37% solution in water) were added.

Results

The TEM images of different batches of the Au NR synthesis by the Ye and Murray's method are shown in figure 2.2. The length, width and aspect ratio are shown in table 1. Even though the Au-NR001 until Au-NR006 were made using the same concentrations of chemicals, there were variations in their size. This can happen as gold synthesis is sensitive to small changes, such as small differences in temperature or stirring speeds. It is difficult to prevent these small changes as they happen due to the apparatuses used. The TEM images show that there are not many shape impurities. The absorption spectra show that the rods with a higher aspect ratio have a higher longitudinal LSPR peak as explained in the introduction. Au-NR004 and Au-NR006 almost have the same aspect ratio, but the length and width of Au-NR006 are almost 10% lower than that of Au-NR004. This proves that the LSPR peak position corresponds with

Sample	Length (nm)	Width (nm)	Aspect Ratio	λ_{max} (nm)
Au-NR001	75.8 (±9.03)	28.7 (±3.91)	2.72 (±0.45)	729
Au-NR002	67.4 (±12.2)	31.0 (±5.85)	2.19 (±0.56)	652
Au-NR004	71.4 (±8.17)	23.8 (±3.59)	3.09 (±0.58)	717
Au-NR006	63.2 (±6.76)	20.7 (±2.52)	3.08 (±0.48)	718
Au-NR007	80.5 (±12.7)	14.7 (±2.26)	5.54 (±1.06)	957

Table 1: The length, width and aspect ratios of the different gold batches shown in figure 2.2. The particles are measured by hand using ImageJ over 100 particles. The ± shows the standard deviation in nanometers. The table also mentioned the wavelength at which the absorption was at the maximum.

the aspect ratio and not with the length or volume of the Au NR [14, 24]. The correlation between the LSPR peak and aspect ratio can be seen in figure 2.3.

There seems to be a linear correlation between the wavelength and the aspect ratio in the following way

$$LSPR = 91.51\Gamma_G + 437.8 \tag{2.1}$$

with the LSPR peak in nanometers and Γ_G the aspect ratio of the gold nanorod. This formula is similar as mentioned in the literature [58], however it is not exactly the same. The reason for this can be explained by small changes in the experimental parameters, such as the concentration of CTAB. The capping agent used and the concentration of capping agent have a strong influences on the dielectric constant of the nanoparticle [16]. Therefor it is difficult to directly compare the data from the literature (which is calculated without the solvent effect) and the experimental data presented here (which can not be measured without the solvent effect) [58]. However, since the CTAB concentration is constant for all the sample, the clear linear trend the literature predicts is evident. Except for the value of AU-NR001. This can be explained by a small error in the synthesis; during the last washing step, the sediment

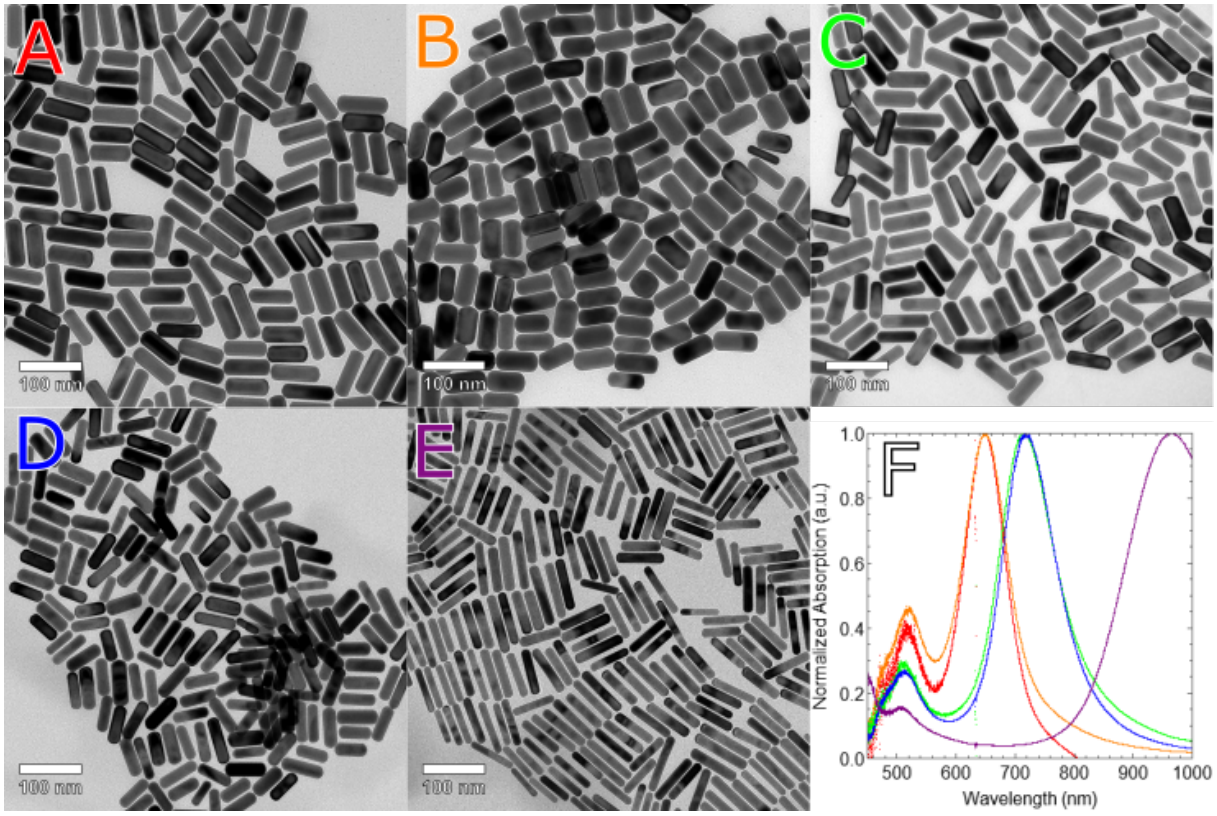

Figure 2.2: A-E: TEM images of Au-NR synthesized using the Ye & Murray's method (batches Au-NR001, 002, 004, 006 and 007 respectively.).For A-D the aimed AR was 3 and for E the aimed AR was 6. F: the normalized absorption spectra for the five batches. The colour of the letter corresponds with the colour of the absorption spectra

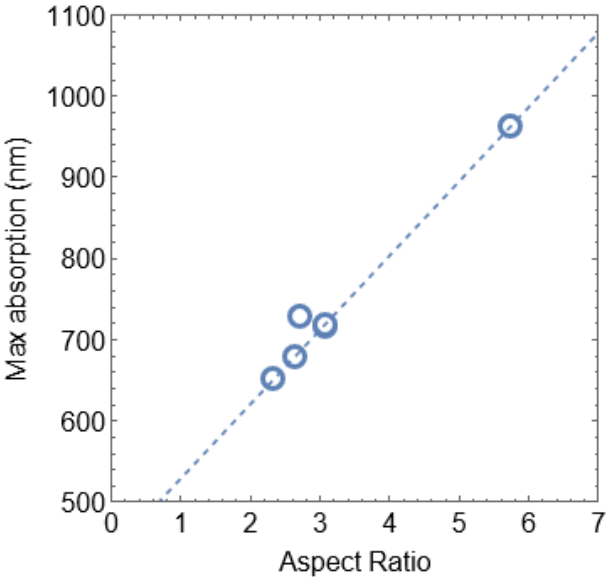

Figure 2.3: The correlation between the aspect ratio of the gold nanorod and the wavelength with the maximum absorption

got disturbed while discarding the supernatant. This resulted in much more of the supernatant being left at the end of the clean-up step (around 5 mL instead of less than one). Normally the vial used to store the gold nanorods is almost completely filled with a CTAB solution (35 mL of 5 mM). The leftover supernatant resulted in that only 30 mL effectively lowering the CTAB concentration by around 14%. The effect of the CTAB concentration towards the LSPR peak has also been shown experimentally [59]. This small error shows how sensible the absorption spectrum of these gold nanorods is for small changes in the ligand concentration. This makes it hard to compare the absorption spectra of one synthesis with the other. Small changes on the dielectric constant, such as the CTAB concentration or a different shape can have a big difference in the precise shape of the absorption spectrum [16, 24].

By using the Ye & Murray's method, Au-NRs with different aspect ratios, with almost no shape impurities, could be synthesized. However, since the goal is to obtain gold nanorods with an aspect ratio of at least 8, it would be better to use a different method (Chang & Murphy's method [17]) as the current used method is not suitable for synthesizing gold nanorods with an aspect ratio bigger than 6 [44].

2.3 Synthesis of Gold Nanorods via the Chang & Murphy's method

To be able to obtain a higher aspect ratio of gold nanorods the Chang and Murray's method [17] was used. This method has been reported to be able to create gold nanorods up to an AR of 10.8. In this method, hydroquinone (a weak reducing agent) has been used instead of AA used by Ye and Murray [44]. This slows down the overall reaction [33], which results in smaller rods (around 8 nm. Also, an increased volume of seed solution was added to the growth solution. This method also increases the concentration of HCl, resulting in a lower pH. Further, NaOL was not used for this synthesis method. Overall, these differences will result in smaller rods (up to a width of 8 nm) with around the same length, meaning that they have much higher aspect ratios.

Synthesis

Preparation of the seed solution: In a 40 mL vial, a mixture of 9.50 mL CTAB (100 mM), 400 µL water and 100 µL HAuCl4 (50.0 mM) was prepared and placed in a water bath of 27 °C stirring at 400 rpm. After 10 min a solution of 10.0 mM $NaBH_4$ dissolved in cold (4.0 °C) 10.0 µM NaOH was prepared. Within 30 s of preparing the 10.0 µM solution 460 µL of this $NaBH_4$ solution was added to the seed solution while stirring at 1200 rpm Then the seed solution was aged for at least 2 h.

Preparation of the growth solution: Three batches of 8.00 mL 100 mM CTAB, 400 µL water and 100 µL $HAuCl_4$ (50.0 mM) was prepared in 40.0 mL glass vial. Each batch was placed in a water bath of 27 °C stirring at 400 rpm. 40.0 µL 0.100 M$AgNO_3$ was added to each batch. After 5 min 25.0, 36.0 or 45.0 µL

1.00 MHCl was added to each batch respectively After 15 min the stirring speed was increased to 700 rpm and 500 µL 100 mM hydroquinone was added to each growth solution. After the growth solution turned colourless 2.00 mL of the seed solution was added to each batch of growth solution. After that, the growth solution was stirred for 2 minutes at 500 rpm and aged overnight before washing.

Washing: The solution in each of the three vials was transported to three 5 mL Eppendorf cups. Each was centrifuged for 25 min at 16 000 rcf. After centrifuging, the supernatant looked completely transparent. This is not good as this means that all the gold, including the shape impurities are in the sediment. One of the reasons for washing is to separate the impurities from the nanorods, the sediments were redispersed with water and centrifuged again with a lower speed (6000 RFC) for 20 min. This time, the supernatant did have a colour. A 5.00 mM CTAB solution was prepared. The supernatant of each Eppendorf cup was transferred to 8.00 mL vials and stored. The sediments were redispered with 5.00 mL 5.00 mM CTAB and stored as well.

Results

The TEM images and VIS-NIR spectra of gold nanorods synthesized by the Change & Murray's method are shown in Fig 2.4. Table 2 summarizes the length, width, aspect ratio and at which wavelength the absorption of the maximum and how much HCl was added to each batch. The maximum LSPR peak of Au-NR010 could not be determined as it is above 1200 nm. Here the absorption of water gives trouble to determine the exact wavelength of the LSPR peak. The frequency for the hydrogen bonds between the water molecules lies around this area [60]. A big problem in optical extinction spectroscopy is that

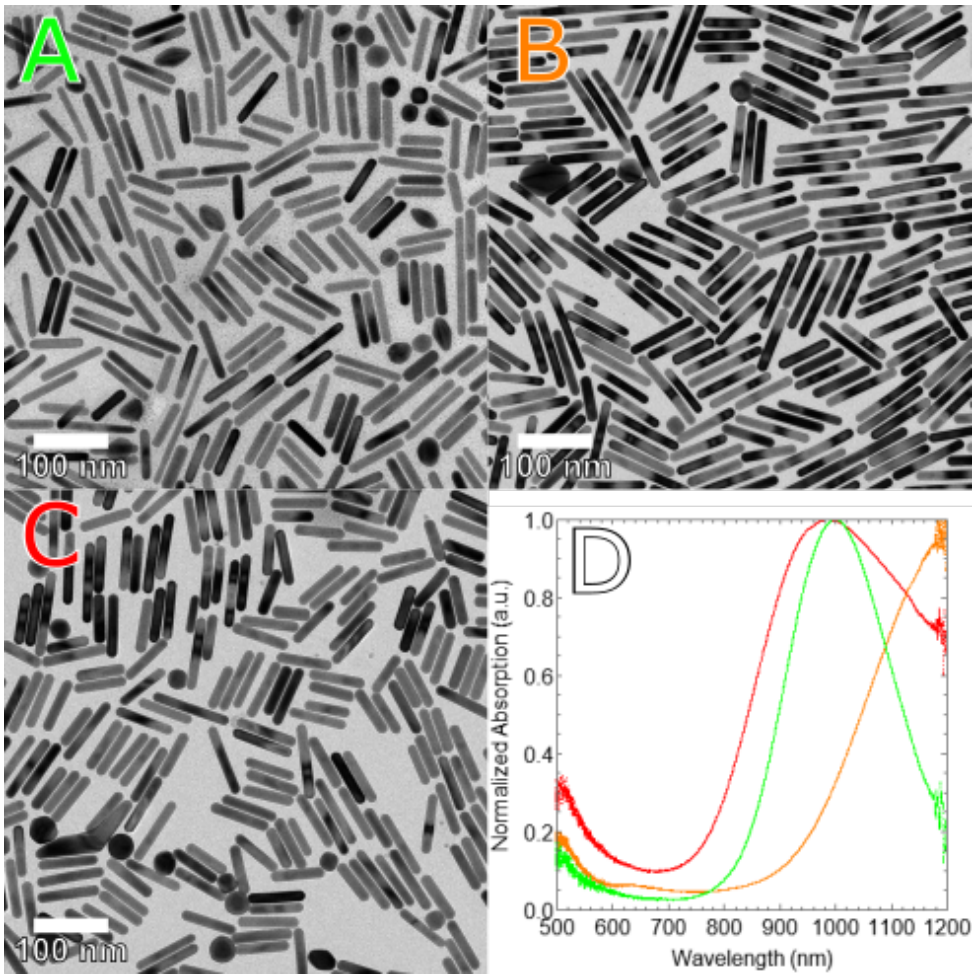

Figure 2.4: A-C: TEM images of Au-NR's synthesized using the Chang & Murphy's method (batches Au-NR009, Au-NR010, Au-NR011). Their length, size and AR can be found in table 2. D: the normalized absorption spectra for the three batches. The colour of the letter corresponds with the colour of the absorption spectra.

Sample	HCl added (µL) (1.0 M)	Length (nm)	Width (nm)	Aspect Ratio	λ_{max} (nm)
Au-NR009	25	85.3 (±26.83)	12.9 (±2.23)	7.16 (±2.91)	989
Au-NR010	36	99.6 (±30.2)	12.4 (±1.47)	8.30 (±2.81)	>1200
Au-NR011	45	84.7 (±22.5)	15.6 (±1.47)	5.44 (±1.69)	970

Table 2: The length, width and aspect ratios of the different gold batches shows in figure 2.4. The particles are measured by hand using ImageJ over 100 particles. The values between the brackets show the standard deviation in nanometers. The wavelength at which the absorption is the maximum is also mentioned.

the absorption and extinction of these hydrogen bonds between the water molecules are very flexible as they depend on distances between the molecules and are a completely different type of bond compared to covalent bonds. Because of this, these interference can not be filtered out in any way. Running an blanco sample for example will not fix this problem. The noise of the water bonds becomes much to intense at 1200 nm to measure anything else [17]. This is also the reason why the data points at the far right side aren't forming a nice line. The water is already interfering a bit, creating a lot of noise.

Au-NR009 and Au-NR010 were made in a similar way as the nanorods in the paper by Chang and Murray with AR 9.6 and 10.8 (mentioned in table 2 of [17]). The length and width of the gold nanorods mentioned in the paper are smaller, but the AR is higher than the gold nanorods synthesized here. It is unclear why this is the case. However, this is also the case for the rods synthesized using the Ye & Murray's method. An explanation for this could be that the Murray group has better control over the temperature. The heaters at the SCM group are not very precise, while literature shows that fluctuations in temperature lead to a lower AR [61]. It is also possible that both papers have neglected to mention a small step in the synthesis which has a great influence on the control of the AR (note that both papers are from the same group). However, as these papers are cited many times, this seems unlikely. However, it is known in the SCM group that the AR of the gold nanorods are usually lower what is reported for the Ye& Murray method [62, 63].

For the batch Au-NR011, 45 µL of HCl (1.0 M) was added. This is higher than the maximal amount added in the Chang and Murray paper [17]. An increasing the amount of HCl will lower the pH. This will lead to a difference in reaction potential between the hydroquinone and the gold atoms, resulting in a higher aspect ratio. however, if the pH gets too low it can weaken the reduction properties of hydroquinone. This could explain why the aspect ratio of Au-NR011 is lower than expected [64]. Another theory is that there is an interesting interplay between the silver ions and the Au-Cl_xBr_y complexes. Increasing the amount of HCl, increases the amount of Cl^--ions, which can stabilize the AgCl-comlexes without the destabilisation of the Au-Cl_x complexes. This prohibits the further growth of the nanorods [17]. This can also explain why the length is lower than of Au-NR009. It seems that further increasing the amount of HCl will not lead to gold nanorods with a higher aspect ratio.

2.4 Determining the gold concentration

The concentration of gold nanorods was determined as reported in [65]. The values can be found in table 3. For the calculations, the Au NRs were considered as a cylinder with spherical ends and so, it makes the volume of the rod the following:

$$V_{rods} = \frac{1}{4}\pi W^2(L - W) + \frac{1}{6}W^3 \tag{2.2}$$

with L the end-to-end length of the rods and W the width of the rod. The volume a gold atom takes within a solid bulk gold compound is [65]:

$$V_{Au} = \frac{1}{4}a^3 = \frac{1}{4} * 0.408\,\text{nm}^3 \approx 0.0169\,\text{nm}^3 \tag{2.3}$$

with a being the crystalline length of gold atoms in a solid. This can be used to estimate the amount of gold atoms with one gold rod (by dividing 2.2 by 2.3). The gold nanorod concentrations can then be

estimated by dividing the amount of concentration of reacted gold(III) ions by the number of gold atoms per nanorod. This gives the following equation:

$$c_{rods} = \frac{\alpha * c * V * N_a}{N_{atoms}} \tag{2.4}$$

were α is the ratio between how much of the gold(III) ions reacted, c is the molar concentration of the gold precursor, V is the end volume, N_a is Avogadro constant and N_{atoms} is the number of gold atoms per rod. In the Ye & Murray's method there is 80.0 µM of ascorbic acid in solution (1.25 mL of 64 mM concentration is added) and there is 250 µM of gold(I)atoms (5 mL of the 50 mM $HAuCl_4$, where the gold is reduced to Au(I)). As each ascorbic acid molecule is able to reduce two gold atoms to gold(0), this means that 64% of all the gold(I) will be reduced. This makes $\alpha = 0.64$ for this synthesis. In the Chang & Murphy's method, there is 50 µM hydroquinone (500 µL of a 100 µM concentration is added) for 5.0 µM gold(I) atoms, so it can be assumed that all of the gold(I) atoms will be reduced, resulting in a α of 1.0.

Using equation 2.4 the concentration of rods can be calculated. The concentration for a few batches is listed in table 3. For the Ye & Murray's method, the end volume was always 40 mL which then resulted in a concentration of around 10^{-9} M. For the Chang & Murphy's method, the end volume was 5 mL, which results in a concentration of around $8*10^{-8}$ M, but for later syntheses (starting from Au-NR012A), the end volume of 1.1 mL was chosen to make the end concentration more in line with that of the Ye & Murray's method.

Sample	Synthesis used	Aspect Ratio	End volume mL	Estimated concentration M
Au-NR001[a]	Ye & Murray's	2.72 (±0.45)	40	$1.13*10^{-9}$
Au-NR004[a]	Ye & Murray's	3.1 (±0.58)	40	$7.35*10^{-9}$
Au-NR006[a]	Ye & Murray's	3.1 (±0.48)	40	$1.06*10^{-8}$
Au-NR007[a]	Ye & Murray's	5.7 (±1.06)	40	$1.65*10^{-8}$
Au-NR008[b]	Chang & Murphy's	7.4 (±2.18)	5.0	$8.03*10^{-9}$
Au-NR012A[b]	Chang & Murphy's	8.25 (±2.20)	1.1	$7.63*10^{-9}$
Au-NR012C[b]	Chang & Murphy's	8.50 (±3.50)	1.1	$6.31*10^{-9}$

Table 3: The calculated gold nanorod concentration for various batches of gold nanorods.

2.5 Scaling up the Chang & Murphy's method

The yield of gold nanorods by the Chang & Murphy's method is around 40 to 80 times lower than that of the Ye & Murray's method (see table 3 to compare concentration and volume) due to the growth solution being way smaller (10 mL scale instead of a 500 mL scale). Also, for the Chang & Murphy's method much more seed solution is used (20% instead of 8% (V/V)). The problem with this is that if one wants to store the gold nanorods made by the Chang & Murphy's method at the same concentration as the Ye & Murray's method, the end volume becomes only 0.5 mL, which is way lower than the 40 mL of the Ye & Murray's method. It is important that the concentration of the gold nanorods are the same when doing the silica coating to be able to compare the results of different experiments. More on this in the next chapter. The big problem with the low yield is that many batches of gold nanorods are needed to perform the experiments on the silica coating. To overcome this problem, it was tried to scale up the Chang & Murphy's synthesis.

Scaling up the seed solution

The first idea that was tried was to increase the scale of the seed and growth solution to the 100 mL-scale, thus increasing the scale by a factor 10. This was done by increasing the volumes accordingly while keeping the concentrations the same. This synthesis was unsuccessful; no gold nanorods were formed. It is thought that the amount of $NaBH_4$ added to the seed solution (4.60 mL) wasn't able to diffuse quickly enough in the larger glassware. Normally, when $NaBH_4$ is added to the seed solution some quick changes in the colour can be seen in the seed solution; brown-purple for a second, colourless and then slowly brown. In this synthesis the brown-purple colour change was visible, but not through the whole solution,

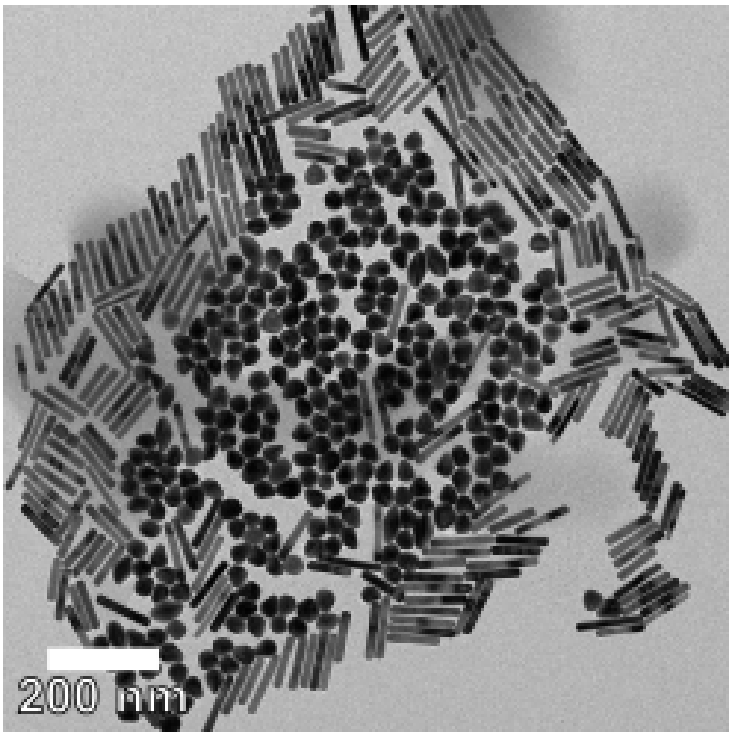

Figure 2.5: The TEM image of gold batch Au-NR015. Details on the sizes are shown in table 4

only the middle part. After that, the whole solution became pale yellow and stayed that colour. When this seed solution was added to the growth solution, no rods were formed.

The pale yellow colour of the seed solution is likely a mix of the colourless Au(I) and the orange-yellow Au(III). The brown-purple colour is probably the formation of really small Au(0) clusters. However, because there are a lot of Au(III) atoms still present, it can be that the small Au(0) clusters are oxidized back to Au(I). Normally this should not happen as the small Au(0) clusters are stable. However, if there is a lot of Au(I) and Au(III) present and CTAB is involved, this could happen [66].

What happens in the up-scaled samples is that the Au(III) is reduced to Au(0) by the $NaBH_4$. The Au(0) atoms will quickly form really small colloids, which gives the brown colour. However, not all the Au(III) is reduced, which can be seen by the fact that the yellow colour remains. The remaining Au(III) atoms can, with help of the CTAB present, oxidise the colloidal Au(0) to Au(I) [66]. Since Au(I) is colourless and Au(III) is yellow, the pale yellow colour is a mixture of Au(III) species and Au(I) species. In the end, the synthesis failed. Even though there is the formation of seeds, evident by the brown color, all the seeds that do form will dissolve and turn back into Au(I) at the end of the 30 min waiting window. This problem could be solved by adding more $NaBH_4$. However, literature reports that increasing the $NaBH_4$ concentration decreases the aspect ratio [67]. The same paper shows that increasing the gold concentration could counteract this decrease of aspect ratio. But increasing the gold concentration would also mean that more Au(III) needs to be reduced, so probably gives the same problems. It is also noted in the literature that the focus on the growth solution instead of the seed solution to change things about the synthesis is much more likely to give good results [49].

Scaling up the growth solution

Due to the problems mentioned earlier, further scaling of the seed solution could not be done. However, some other path was tried. In the normal procedure, only 2.0 mL of the seed solution is used, while the whole seed solution consisted of 10 mL, the growth solution could be scaled up to 50 mL without the need for scaling up the seed solution. To do this a 100 mL round bottom flask was used instead of the 40 mL vials. The result of this batch is shown in figure 2.5. The sizes are shown in table 4. Two things are evident. First, the number of shape impurities increased drastically. Second, the aspect ratio was lower than the standard procedure (for example Au-NR010). It would be simple to think that the lower aspect ratio is a direct consequence of the more shape impurities; more gold in the shape impurities,

Sample	Length (nm)	Width (nm)	Aspect Ratio
Au-NR015	107.8 (±20.6)	16.6 (±2.07)	6.59 (±1.61)

Table 4: The length, width and aspect ratios of Au-NR015 in figure 2.5. The particles are measured by hand using ImageJ over 100 particles. The values between the brackets show the standard deviation in nanometers.

less gold in the rods and thus shorter rods. However, this is not the case. The length of the rod is higher, the same as the width. Something else must be the case. Due to the larger scale, the kinetics of the reactions have changed. It could be that the higher volume creates a less homogenized mixture. Presumably locally increased CTAB concentrations results in the formation of small micelles. These smaller micelles no longer contribute in the same way that free CTAB does, ergo this effectively lowers the CTAB concentration that could react with the gold. A lower CTAB concentration results in bigger nanorods with more shape impurities [61].

Since changing the kinetics of the reaction could mean that different concentrations of CTAB of different stirring speeds would be necessary, finding out why exactly the rods had a lower AR (or to be more precise how to perform the synthesis with the higher AR) would lose a lot of time. Another way to scale up the synthesis is using five different growth solutions of 10 mL similar to the usual synthesis method. But this can also be seen as doing five different syntheses at the same time.

2.6 Problems with the Chang & Murphy's method

Table 5 shows the length, width and aspect ratio of 27 different batches of gold nanorods synthesized via the Chang & Murphy's method as described in section 2.3. For all these batches, the experimental parameters were the same (except Au-NR008, Au-NR009, Au-NR011 and Au-NR015, as explained in the subscript of the table). Thus in theory, the dimensions of these gold nanorods should all be the same. However, there is a lot of variation in the length and width of the nanoparticles. It is unclear why there is such a large difference. However, some theories are considered below.

First a small note. Sometimes different gold nanorods batches were synthesized from the same seed solution. These batches have the same number, but a different letter at the end (thus for example Au-NR019A and Au-NR019B). Au-NR009, 010l and 011 are also synthesized from the same seed solution (but differ in their experimental parameters).

Most of the variation seems to be in the length of the gold nanorod, which could have a value between 27.4 till 104 nm. For the width, this variation seems a bit less, as it seems to be two groups; it seems that the width of the rods is about 7 nm or about 12 nm. According to the Chang & Murphy's paper, the length and width of the rod should be 93.1 ± 18.3 and 8.7 ± 1.0 nm respectively.

It is interesting that there were two distinct sizes for the width and not a gradient of different values as is the case with the lengths of rods. Even though the same procedure was used for all the synthesized gold nanorods, there could be small differences in the particle dimensions from small syntheses variations that could happen from time to time (such as the temperature of the room and time between steps) or the effect of chemicals over time (such as chemicals ageing over time). These small synthesis variations could result in nanorods which are slightly bigger or smaller than the aimed size. However since they are random (nothing is deliberately changed; sometimes the room is a little bit hotter and sometimes a little bit colder), the values should be random. For the length of the rods, this seems to be the case. However, for the width, it seems that the value is first around the 12 nm, then around 7 nm and then for the last batches again to 12 nm (or even 19 nm at the very end). This could suggest that error has something to do with something more systematical (e.g. change of batch of chemicals). As of right now, it is unclear what is causing these large differences between batches. However, here two different theories will be discussed, which could be an explanation; the effect on $NaBH_4$ and NaOH, which could possibly explain the variations.

The role of $NaBH_4$

One reason the rod formation wasn't working probably could be a degradation of $NaBH_4$. As mentioned before, when the $NaBH_4$ is added a large colour difference is visible. In the end, a slightly brown colour should form. If the solution at the end is completely transparent or pale yellow, then the reduction

Sample	Length (nm)	Width (nm)	Aspect Ratio
Reported by C&M	93.1 (±18.3)	8.7 (±1.0)	10.8 (±2.8)
Au-NR008[a]	54.5 (±10.1)	7.67 (±1.67)	6.91 (±2.18)
Au-NR009[a]	85.3 (±26.8)	12.9 (±2.23)	7.16 (±2.91)
Au-NR010	99.6 (±30.2)	12.4 (±1.47)	8.30 (±2.81)
Au-NR011[b]	84.7 (±22.5)	15.6 (±1.47)	5.44 (±1.69)
Au-NR012A	79.6 (±15.1)	9.93 (±1.86)	8.11 (±2.20)
Au-NR012B	63.2 (±19.0)	11.47 (±1.82)	5.42 (±1.83)
Au-NR012C	88.2 (±26.2)	10.34 (±1.46)	8.50 (±3.50)
Au-NR015[c]	104.1 (±20.6)	16.7 (±2.07)	6.38 (±1.61)
Au-NR018A	40.6 (±12.4)	7.15 (±1.35)	5.82 (±1.82)
Au-NR019A	27.4 (±10.1)	6.35 (±1.15)	4.28 (±1.75)
Au-NR019B	27.7 (±7.85)	6.93 (±1.35)	4.02 (±1.26)
Au-NR019C	41.9 (±9.43)	7.61 (±1.10)	5.51 (±1.54)
Au-NR019D	36.9 (±10.5)	6.67 (±1.34)	5.44 (±1.76)
Au-NR019E	30.7 (±7.77)	7.56 (±1.26)	4.20 (±1.13)
Au-NR020A	54.2 (±11.6)	8.37 (±1.30)	6.43 (±1.70)
Au-NR020B	45.3 (±10.6)	7.51 (±1.33)	5.81 (±1.65)
Au-NR020C	58.5 (±14.3)	7.70 (±1.57)	7.52 (±2.23)
Au-NR020D	53.4 (±15.0)	7.92 (±1.26)	6.65 (±2.62)
Au-NR020E	52.4 (±12.8)	7.87 (±1.16)	6.62 (±2.26)
Au-NR021A	37.4 (±8.74)	7.56 (±0.92)	5.00 (±1.27)
Au-NR021B	53.5 (±9.71)	7.82 (±1.06)	6.93 (±1.48)
Au-NR021C	39.8 (±13.6)	7.78 (±1.01)	5.07 (±1.90)
Au-NR021D	37.8 (±9.87)	7.28 (±2.26)	5.12 (±1.19)
Au-NR021E	45.0 (±21.4)	7.06 (±2.00)	6.41 (±2.99)
Au-NR022	80.0 (±30.2)	11.6 (±2.21)	6.97 (±3.54)
Au-NR027	69.1 (±25.4)	13.9 (±3.11)	5.07 (±3.23)
Au-NR033D	81.1 (±38.0)	19.1 (±3.88)	4.29 (±3.01)

Table 5: [a]25 µL HCl(1.0 M) was added instead of 36 µL; [b]45 µL HCl(1.0 M) was added instead of 36 µL; [c]created at a 50 mL scale instead of 10 mL. The length, width and aspect ratios of various batches of gold nanorods created with the Change and Murray's method. The particles are measured by hand using ImageJ over 100 particles. The values between the brackets shows the standard deviation in nanometers.

is unsuccessful; no seeds are formed and all the Au(0) formed would oxidize back to Au(I) due to the presents of CTAB [66].

During the experimental part of the thesis it was noticed that for the experiments done in the later months of the thesis, there was a higher chance of a failed synthesis than in the early months of the thesis. In the beginning, most of the seeds solution would have been reduced correctly. Sometimes it didn't, but then a new seed solution was created, which would reduce correctly after the addition of $NaBH_4$. A few months later, it was almost standard that the first time the seed solution was prepared the reduction didn't go correctly and a second or even third batch of seed solution was needed before a successful reduction took place. This suggests that the bottle of $NaBH_4$ has gone bad over time.

Since $NaBH_4$ reacts with water in the air, it needs to be stored under nitrogen flow. Even though this is the case in the SCM lab, the bottle used was opened in 2015, meaning that it is over six years old at the time of writing. As every time the bottle is used, a few molecules get oxidized. So if the bottle is that old, then at a certain point a significant portion is oxidised that it becomes noticeable. Also, it was noted that the water pressure in the nitrogen box was higher than usual in June 2021, which was between the time Au-NR015 and Au-NR 18 were made. It could be that this unusual high water pressure aged the old bottle of $NaBH_4$ so significantly that the amount of unreacted $NaBH_4$ in the synthesis significantly changed, resulting in a higher chance of the experiment failing. Or when seeds would form, it would have been at a lower concentration. This would then result in bigger gold nanorods [61].

It is reasonable to think that the old bottle of $NaBH_4$ could explain the random variations in the result of these syntheses. If the $NaBH_4$ in the bottle is partly oxidized, then not only a lower amount of unreacted

$NaBH_4$ is added to the synthesis than precibed by the protocol, but the amount will also be random[3]. When the molar ratio between $NaBH_4$ and $HAuCl_4$ in the Chang & Murphy's synthesis is calculated, one can see that there is an excess of $NaBH_4$ of 23% (M/M%)). This means in theory 23 molar percent of the $NaBH_4$ doesn't need to react with the gold atoms, for all the gold atoms to still be reduced. This isn't a big excess, realising that $NaBH_4$ will also react with the solvent. So if the $NaBH_4$ is already partially oxidized in the bottle, the chance of not adding enough $NaBH_4$ seems very reasonable. This then would result in less Au(O) available, resulting in less to no seeds.

To test this theory a new bottle of $NaBH_4$ was ordered. Due to delivery problems, $NaBH_4$ of a different company was ordered which is only 98% pure instead of 99% pure. This difference may not look much, but as mentioned earlier, the impurities in CTAB can make or break the synthesis [53], thus it could be that the impurities in $NaBH_4$ could influence the syntheses as well. And unfortunately, it seems that this is the case. There were four attempts at reducing the seed solution with the new $NaBH_4$ and all failed; the seed solution turned yellow and not brown (see also figure A.2). It is unclear which impurity in the bottle results in the failed synthesis. Most of the 2% impurity is magnesium carbonate, which is added to the $NaBH_4$ as an anticaking agent. It is known that a ratio between CTAB and magnesium carbonate can influence the growth of mesoporous magnesium silicate. The magnesium carbonate interacts with the CTAB, affecting the micelle formation which influences the formation of the magnesium silicate [68]. As CTAB is influential in the stability of the gold seeds, it is reasonable to think that maybe the magnesium carbonate prohibits the formation of the gold seeds. However, more research is needed to prove this theory.

Another synthesis was done where 460 µL of freshly prepared 20 µM $NaBH_4$ (of the new bottle) was added to the seed solution instead of the normal 10 µM, thus doubling the amount of $NaBH_4$. This solution was still prepared in 100 mM NaOH solution to limit the number of changes. When the 20 µM $NaBH_4$ solution was added, the seed solution became way darker than before (see figure A.2). This suggests that way more seeds are formed. Of this seed solution, a batch of gold nanorods was created (see figure 2.6). The mean length and width are 23.0 nm (±(10.9)) and 5.98 nm (±(2.31)) respectively. The mean aspect ratio is 3.83 (±(1.26)). So in conclusion, adding more $NaBH_4$ results in shorter rods. This does agree with literature [61]. The explanation for this is actually pretty simple. More seeds, result in less gold per gold nanorod. Since the rods grow mostly in the length and not much in the width, this would result in much shorter and slightly thinner rods [61]. This would suggest that adding more gold ions, could result in high aspect ratio gold nanorods. However, with the addition of more gold ions, the ratio between the gold atoms and the other chemicals would no longer be ideal. There is another problem with this batch. There is a high amount of shape impurities. There were probably formed due to the more extreme conditions of the seed solution due to the higher concentration of $NaBH_4$. It is also possible that this is an effect of the aforementioned magnesium carbonate. It might be a good idea to wait until a new bottle of the 99% pure $NaBH_4$ can be ordered, to limit the influence of the magnesium carbonate. However, there wasn't enough time for that in the scope of the thesis.

The role of NaOH

Another theory was that maybe NaOH could be a problem. When the $NaBH_4$ solution is prepared, the $NaBH_4$ is dissolved in a cold NaOH (0.01 M) solution. For the synthesis, the NaOH solution wasn't always freshly prepared as it was thought that the (0.01 M) solution would stay stable for at least two weeks. Due to the problems with the synthesis, at a certain point in time, it was chosen to always prepare a fresh solution of the NaOH, to avoid an ageing effect. Au-NR009 until Au-NR015 were all made using the same stock solution of NaOH; Au-NR018A until Au-NR020E were all made using a new NaOH stock solution. After that, for every synthesis, a fresh batch of NaOH was prepared.

It is interesting that the width of gold nanorods all are around the 12 nm for the batches Au-NR009 until Au-NR015 as these are all created from the same batch of NaOH. Then a new batch of NaOH was created which was used for the batches Au-NR018A till Au-NR020E and the width of the nanorods seem to drop to around 7-8 nm. Then for the NaOH batch used for Au-NR021A until Au-NR021E the values are also around the 7-8 nm[4]. Then Au-NR022 and Au-NR027 were also made with the use of the same NaOH solution and again they have a similar width. Even though there seems to be a profound difference in

[3] the reacted $NaBH_4$ will most likely be at the top of the bottle while the unreacted $NaBH_4$ will mostly be at the bottom. Small things like scraping from the top of the bottle or the shaking of the bottle itself due to walking e.g. will effect how much of the reacted and unreacted amount of $NaBH_4$ will be within the 100 mM solution.

[4] note that these were all made from the same seed solution

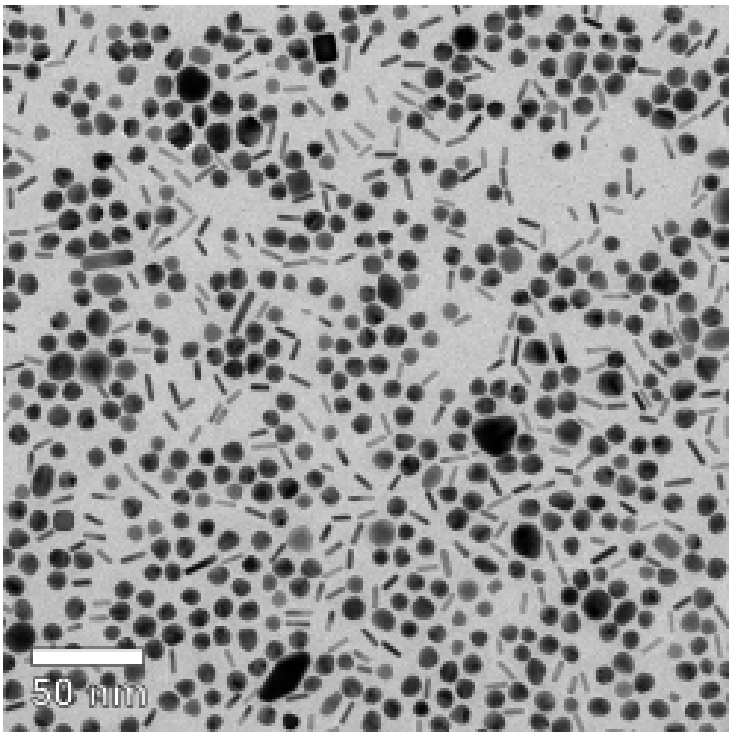

Figure 2.6: A TEM image of the batch Au-NR039. The mean length and width are 23.0 nm (±(10.9)) and 5.98 nm (±(2.31)) respectively The mean aspect ratio is 3.83 (±(1.26)

width from NaOH batch to NaOH batch, this difference isn't that profound for the length.

An explanation for the variation between the NaOH batch could be that the concentrations were not precisely correct. This would mean that the pH is slightly higher or lower in the seed solution than it should be. As the seed solution is added to the growth solution, a difference in pH in the seed solution would result in a difference in pH in the growth solution. As mentioned before, the pH is important for the symmetry-breaking step. The pH will influence at which point in the growth of the nanoparticle it will happen [56]. This will then have a profound impact on the width of the particle [56]. So that could explain the difference. However, only a little (460 µL) of the NaOH solution is added to the seed solution. In the end, the 10 µM NaOH will only be 0.8% of the total growth solution, thus if the 10 µM solution was a 15 µM solution by an experimental error (which is a large error to make without noticing), this would increase the NaOH concentration in the growth solution by around 40 nM. Does this small amount of base change the pH strongly enough against the 4.5 mM concentration of hydroquinone or 3.2 mM HCl that was added? Probably not. It is however curious that the variation in width is so profound with the change in the NaOH batch.

Another theory is that a variation in NaOH would affect the $NaBH_4$ that react with $HAuCl_4$. As mentioned before, the $NaBH_4$ is dissolved in NaOH to slow down the reaction with H^+. If accidentally the concentration of NaOH is different, then the reaction rate of $NaBH_4$ in solution is different, thus also the amount of $NaBH_4$ that reacts with the $HAuCl_4$ giving similar problems as described above (but on a much smaller scale as the pH should only be slightly off). However, a change in seed concentration mainly influences the length of the rod and not the width [61]

Further, a difference in pH could possibly lead to the formation of a differently shaped seed. Different seeds can yield in distinct lengths and widths [54], so theoretically this could explain the profound difference. However, since the difference in length isn't clear and seems to have a more random effect than it is the case with the width of the rods, and different seeds give distinct lengths *and* widths, this theory seems less likely.

So in the end, it isn't clear why the synthesis gives such a large variation in rod sizes. It could be that one or more of these theories is correct, but there isn't strong evidence. So it could be that the reason is something completely different. It is really unfortunate that the error with the gold nanorods synthesis could not be found as this servery limits the number of gold nanorods available for the silica coating

experiments.

3 Silica-coated gold nanorods

3.1 Theory of silica-coated gold nanorods

The use of silica for coating of the gold nanorods

As mentioned in the introduction, the goal of this thesis was not only to make gold nanorods, but also to coat them with a porous layer of silica oxide. There are a few reasons to do this. As mentioned before, the silica layer will shield the strong van der Waals attraction of the gold nanorods. This will prevent aggregation and helps with the self-assembly of the gold nanorods (see also figure 1.12). Another reason is that a silica shell around the gold nanorod improves the thermal stability of the particles [39, 69, 70]. Heating them could lead to the rods becoming more spherical [69, 71]. The shell increases the thermal stability as it lowers the surface energy of the gold nanorod. It also prevents the migration of the surface atoms [39, 69, 70]. Further, the silica shell will also prevent the gold from oxidizing or other surface reactions that could influence the plasmonic effect of the gold nanorod [69].

The gold nanorods are not coated with a solid silica layer, but with a mesoporous shell (pores with a diameter in the order of a few nanometers). This leaves the gold surface accessible for chemical treatments. The mesoporous structure actually helps in the mass transport of chemicals [39]. This makes it possible to create bimetals rods to enhance the SERS (by using silver) or for catalytic purposes [39, 65].

The use of silica oxide (SiO_2) further makes the gold nanorod more biocompatible. It also reduces toxicity, as CTAB is no longer needed to make the particles dispersed in water. Further, the silica layer can also be used to attach other molecules to it for further functionalization if that would be necessary for future applications [72].

The mechanism of growing silica layer over Au NRs

The silica source in the syntheses is the commonly used tetraethyl orthosilicate (TEOS). In the presence of water, TEOS will condense into SiO_2 and ethanol. In the synthesis, NaOH is added to increase the pH to 11 to boost the reaction speed. The higher pH also increases the solubility of SiO_2 [73].

Because gold has a weak affinity with SiO_2, it is impossible to graft the SiO_2 directly on the gold nanorod. This problem can be overcome by the use of surface polymers [72]. These polymers can react with SiO_2 to form the silica shell. In these syntheses, cetyltrimethylammonium bromide (CTAB) is used. It is already surrounding the gold nanorods, as it is used for colloidal stability [49].

The growth of SiO_2 and CTAB to form the mesoporous silica layer happens in a three-stage mechanism. First, silica oligomerization, where the SiO_2 molecules form small clusters. Then these clusters form together with CTAB small particles. Then these silica-CTAB particles aggregate, forming the silica particle at the end [74,75]. The positively charged head group of the CTAB is what attracts the negatively charged SiO_2 [75]. Since the CTAB molecules strongly localize around the gold nanoparticle, this three-step mechanism will happen around the gold nanorod [75]. This limits the formation of free silica particles [74–76]. Gorelikov and Mutsuura in 2007 were the first to report the synthesis surrounding the gold nanorod with the help of CTAB [76]. Even though the silica formation happens in three stages, it all happens as soon as the TEOS is added to the solution, making it a straightforward single-step procedure [76].

Because the silica oligomers have the tendency to self-nucleate, it is important that the silica concentration doesn't become too high. Because of this, the TEOS is added within time intervals of 30 a 45 min [72,76]. As the CTAB concentration surrounding the gold nanorods is higher than in solution. This resulted that most of the SiO_2-CTAB oligomers will form around the gold nanorods, helping in silica layer formation [76].

The silica layer will grow around the CTAB molecules, but not replace them. Later, the CTAB molecules will be washed away, leaving the mesoporous holes behind [39, 72, 76]. It was reported that varying the CTAB concentration will change the size of the pores [39]. Since the SiO_2 doesn't react with the gold surface, there isn't a covalent bond between the gold nanorod and the silica coating. Because of this, it is possible to etch the gold nanorod without distorting the silica layer. The gold rods could be partly etched away and then it is possible to fill the inside of the silica shell with for example silver, copper, palladium or platinum to improve the SERS of to increase the catalytic effects [39, 65].

3.2 Tuning the silica layer thickness by changing the TEOS concentration

To tune the silica thickness, the first thing tried was to change the concentration of TEOS. Ten batches of the same gold nanorods sample (Au-NR004, for sizes see table 1) were coated with different concentrations of TEOS.

Synthesis

In five 40 mL vials 7.0 mL water, 1.0 mL CTAB (5 mM) and 2.0 mL Au-NR004 ($4.43*10^{12}$ ml^{-1} gold nanorods stored in 5 mM CTAB) were added. The vials were placed in a water bath of 30 °C and stirred at 400 rpm. After 5 min, 100 µL (0.1 M) NaOH was added. A 20% TEOS solution was made by dissolving 200 µL TEOS in 800 µL ethanol (EtOH) (100%). After 30 min 15, 30, 45, 60 and 75 µL of TEOS (20%) were added to five different batches respectively while stirring. To prevent self-nucleation of the silica, 15 µL of the TEOS (20%) was added per time, with 30 min breaks in between. The reaction was performed for 48 h.

After 48 h, the samples were washed one time with water and two times with EtOH (96%). The samples were centrifuged in 15 mL falcon tubes for 15 min at 8000 RCF at 23 °C. Each time the supernatant was discarded and the sediment was redispersed (thus one time in water and two times in EtOH (96%)). The sediments were sonicated and vortexed for a few seconds. In the end, the samples were dissolved in 1.0 mL EtOH (100%). All silica-coated gold nanorod samples were stored in the fridge for stability. The thickness of the silica layers was investigated with the use of TEM.

This experiment was later repeated with five new batches where 10, 20, 30, 40 and 50 µL TEOS (20%) was added, with steps of 10 µL. The rest was kept the same. The gold nanorods used for this batch were also from sample Au-NR004.

Results

In figure 3.1 the thickness of the silica layer is plotted against how much TEOS was added to each batch. At first, the data seems a bit chaotic. However, some conclusions can be drawn.

Looking at the first four data points of the first batch, a clear trend is visible; increasing the TEOS concentration increases the thickness of the silica layer around the Au NRs. This is expected and described

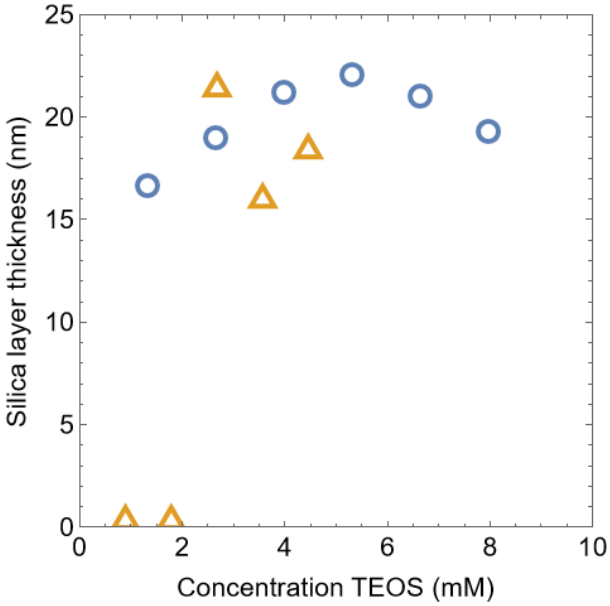

Figure 3.1: A graph showing the initial concentration of TEOS and the thickness of the average silica layer around the gold nanorods (from batch Au-NR004). Two different experiments were performed; the blue spheres correspond with the first batch with steps of 15 µL TEOS added and the yellow triangles correspond with the second batch with steps of 10 µL of TEOS added as described in section 3.2. The thickness of the silica layer was measured by hand using ImageJ for at least 100 particles.

in the literature [72,76,77]. The last two data points have a lower value. The decrease could be explained by the concentration of TEOS surpassing the critical concentration for self-nucleation resulting in silica spheres in the mixture and thus less silica to form the silica layer around the Au NRs. The critical concentration for TEOS to self-nucleated is higher than here is achieved [77]. However, it could be, that when the addition of the TEOS is done, the local concentration of silica is higher than the critical concentration. This could also explain why adding more TEOS would lead to more places where the critical value is exceeded, thus more self-nucleation and thus less silica left to form the layer surrounding the gold nanorods. However, this isn't a strong hypothesis as the samples were stirred properly. Further, the data points corresponding with the second batch don't seem to match with the results of the first batch though; the last three data points of this batch don't show a clear trend and don't seem to have a similar thickness as the data points from the first batch. One could try to see trends with those data points and try to fit a conclusion in them. But that would probably be reading too much into the data as there are only three data points here.

If one conclusions should be drawn from this experiment, it is that controling the thickness of the silica shell by varing the concentration of TEOS isn't an good approach. The minimum thickness of the silica layer seems to differ between the two batches and with the literature [72,77]. Furhter, the silica thickness for the same amount of TEOS for the two different batches differ. There is just to much variation to use these results for any concrete approach of creating thin coated gold nanorods. It is clear from these experiments that it is hard to form thin silica layers. This corresponds with experimental data found in literature [77]. Using this method, a silica layer in the order of 15 nm is formed or not at all. However this thickness of 15 nm is too much for the particles we are trying to create. First of all, if the silica layer is going to have a minimum thickness of 15 nm, then the length of the gold nanorods should be much longer, for example in the ranges of around 200 nm. Secondly, the plasmonic effect is strongly dependent on the distances between the two nanoparticles. It is shown that the plasmonic effect is much stronger for silica-coated gold nanorods with a distance of 3 nm than with silica-coated gold nanorods with a thickness of around 15 nm [74, 78]. Since such thin silica layers don't seem possible with this method, a different method should be sought for the coating of the gold nanorods.

3.3 Tuning the silica thickness with the use of PEG-Silane

Controlling the thickness of the silica layer by just varying the SiO_2 concentration is difficult as can be seen above. A way to gain more control over the thickness of the silica layer would be to be able to stop the reaction after a certain time. 2-(Methoxy(polyethyleneoxy)propyl)trimethoxysilane(PEG-Silane) is a chemical which is able to do this. PEG-Silane is able to terminate the forming of SiO_2-coating which would result in a thinner silica layer. It seems that the PEG-silane molecules are attracted by the silica layer by van der Waals force and electrostatic interactions. These interactions physically block more silica particles to attach to the silica layer, quenching the reaction [73]. By adding the PEG-Silane at different time intervals, silica-coated gold nanorods with different thicknesses could be made. Also, silica layers thinner than 10 nm are possible [72].

The synthesis used here, which uses PEG-Silane to tune the silica thickness is based on the synthesis of Wu & Tracy [72]. This synthesis is similar to the one just in the previous experiment, as they both use the Grelikov method [76]. In the experiment described below two batches of Au-NR006 (see for sizes in table 1) were coated with silica (using 20%-TEOS solution dissolved in ethanol). In one batch 40 µL PEG-Silane was added and in the second no PEG-Silane was added.

Synthesis

In two 40 mL vials 7.0 mL water, 1.0 mL CTAB (5 mM) and 2.0 mL Au-NR006 ($6.38*10^{12}$ mL^{-1}) was added. The vials were placed in a water bath of 30 °C while stirring at 400 rpm. After about 5 min 100 µL 0.1 M NaOH was added. A 20% TEOS solution was made by dissolving 200 µL TEOS in 800 µL EtOH (100%). After 30 min 40 µL of 20 % TEOS was added to each vial. 30 min after that 40 µL of (pure) PEG-Silane was added to one of the vials.

After 48 h, the samples were washed one time with water and two times with EtOH (96%). The samples were centrifuged in 15 mL falcon tubes for 15 min at 8000 RCF at 23 °C. Each time the supernatant was discarded and the sediment was redispersed (thus one time in water and two times in EtOH (96%). The sediments were sonicated and vortexed for a few seconds. In the end, the samples were dissolved in 1.0 mL EtOH (100%). All silica-coated gold nanorod samples were stored in the fridge for stability. The

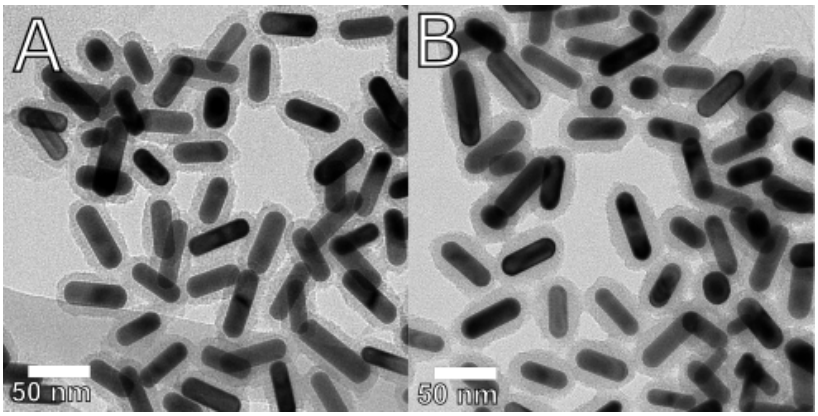

Figure 3.2: The TEM images of two batches of Au-NR006 coated with silica. Figure A shows the result of when PEG-Silane was added after 30 min during the synthesis (average silica thickness of 10.8 nm (±1.39 nm)). Figure B shows the result where PEG-Silane wasn't added during the synthesis (average silica thickness of 13.7 nm (±1.32 nm)).

thickness of the silica layers was investigated with TEM.

Results

Figure 3.2 shows two batches of silica-coated gold nanorods (batch Au-NR006), one with PEG-Silane added during the synthesis and one without the addition of PEG-Silane. The average lengths of the silica layers were 10.8 nm (±1.39 nm) and 13.7 nm (±1.32 nm) for the batches with PEG-silane and without PEG-silane respectively. The stark difference in length shows that PEG-Silane can be used to tune the thickness of the silica layer. The problem right now is that the silica layer formed is still too thick. One could add the PEG-Silane at an earlier time. However, the SiO_2 also needs time to form a nice layer, thus adding it too soon could result in a rough outer layer [72]. A different solution could be the use of a different solvent to dissolve the TEOS as this would change the kinetics of the reaction. This will be discussed in the next section.

3.4 The use of ethanol and methanol to control the silica synthesis

A way to change the kinetics of the reaction is by dissolving the TEOS in an different alcohol. Literature shows that dissolving TEOS in MeOH instead of EtOH will create smaller silica particles [79]. To investigate if this difference is true for the porous silica layer surround the gold nanorods two series of four batches (thus eight in total) of silica-coated Au-NR006 (for sizes see table 1) were synthesized, four with TEOS dissolved in EtOH and four with TEOS dissolved in MeOH. In either of the two series, PEG silane was added at different times - 30, 45 and 60 min after TEOS is added and a batch was without PEG-silane addition for comparison.

Synthesis

In eight 40 mL vials 7.0 mL water, 1.0 mL CTAB (5 mM) and 2.0 mL Au-NR006 ($6.38*10^{12}$ mL^{-1}) was added. The vials were placed in a water bath of 30 °C while stirring at 400 rpm. After 5 min 100 µL NaOH (0.1 M) was added. Two 20 v% TEOS-solutions were made, one with EtOH and one with MeOH, by dissolving 200 µL TEOS in 800 µL EtOH (100%) or MeOH (100%). In 4 vials 30 µL TEOS diluted with EtOH was added and in the other 4 vials, 30 µL TEOS diluted with MeOH was added. At different time intervals (30, 45 and 60 min) 40 µL PEG-Silane was added to the vials (one with EtOH and one with MeOH). In two vials (one with EtOH and one with MeOH) no PEG-Silane was added.

After 48 h the samples were washed one time with water and two times with EtOH (96%). The samples were centrifuged in 15 mL falcon tubes for 15 min at 8000 RCF at 23 °C. Each time the supernatant was discarded and the sediment was redispersed (thus one time in water and two times in EtOH (96%)). The sediments were sonicated and vortexed for a few seconds. In the end, the samples were dissolved in 1.0 mL EtOH (100%). All silica-coated gold nanorod samples were stored in the fridge for stability. The thickness of the silica layers was investigated with the use of TEM.

Results

Figure 3.3 shows the silica thickness vs the time the PEG-silane was added. Here the two batches where no silica was added are plotted at t=200 min, as most of the silica will react within the first 4 hours, [76]. The TEM images are shown in figure 3.4. Based on these results a few things can be concluded. First, adding PEG-silane at different time intervals will affect the silica layer thickness. Based on the data points at t=30, 45 and 60 min it seems that this relationship is linear. However, for the sample without

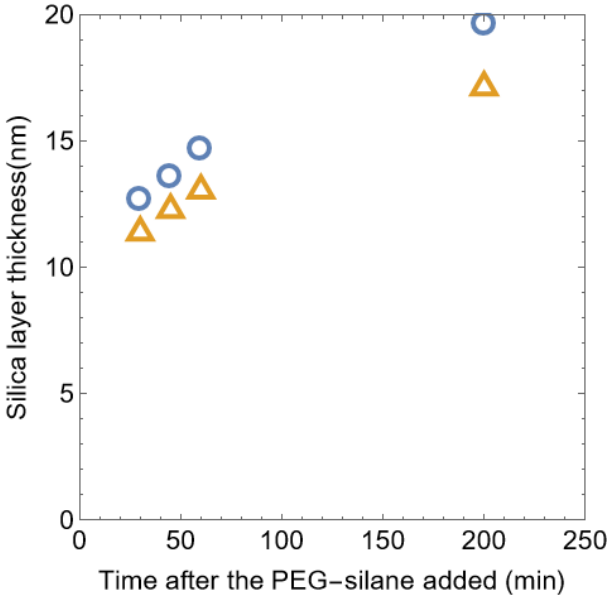

Figure 3.3: The silica layer thickness for gold nanorods (batch Au-NR006) with PEG-Silane added on different time intervals. The batch without PEG added is set at t=200 min. The series where TEOS is dissolved in EtOH is shown by blue spheres and the series where TEOS is dissolved in MeOH is shown by oranges triangles.

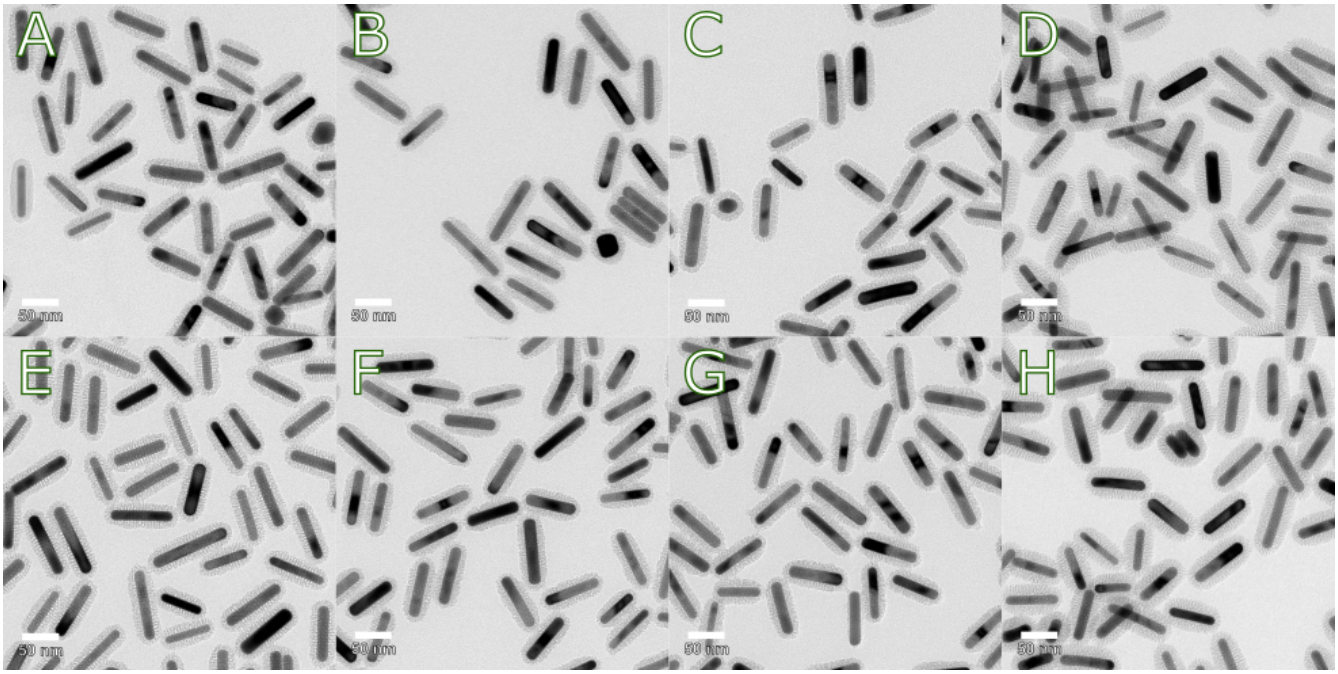

Figure 3.4: TEM images of the silica-coated Au-NR006 (AR of 3.0, $6.38*10^{12}$ particles per mL). TEOS was dissolved in EtOH (A till D) or in MeOH (E till H). PEG-Silane was added at 30, 45 and 60 min (A till C and E till G respectively.). In D and H no PEG-Silane was added. The thickness of the silica layers can be found in figure 3.3

PEG-silane, this linearity seems gone. This corresponds with literature, where indeed, first the silica layer grows linear, but that stops after around an hour [76].

Another observation is that dissolving the TEOS in MeOH resulted in an thinner silica layer. As MeOH is more polar than EtOH, the small silica aggregates with MeOH and CTAB will be more stable than the small silica aggregates with EtOH and CTAB. This stability is due to the higher electrostatic repulsion of the silica aggregates. Because these aggregates are more stable, they are less incline to aggregate with each other to form the silica layer [79]. This slows down the overall reaction rate of the silica layer resulting when the reaction it terminated due to the PEG-silane.

Interestingly enough, in all of the MeOH samples, no self-nucleation of the silica was observed, while all of the EtOH samples did show self-nucleation. This is probably a direct consequence of the stability of the silica aggregates with MeOH. Not only are the silica aggregates less incline to form silica particles around the gold nanorod, they are also less incline to form silica particle some place else (which is also harder to do without the high concentration of CTAB which surround the gold nanorod [74–76]). Self nucleation happens when the local concentration of the oligomers are above a certain threshold. Because the MeOH oligomers are more stable, the local concentration needs to be higher. When the TEOS is added, the local concentration of TEOS is pretty high at the point where the TEOS is added. Because the mixture is stirred, the local concentration of TEOS will change quickly until everything is homogenized. However, this takes a while. This is the reason the addition of TEOS happens in steps with 15 min in between them. It seems that due to the stability of the silica aggregates with MeOH that this threshold isn't breached, but for the silica aggregates with EtOH it is. Still in later batches self nucleation of the silica was observed even though MeOH was used. This shows that the threshold of self-nucleation is close to the experimental parameters.

3.5 Silica coating around Au NR with a higher aspect ratio (>8)

In the experiments mentioned before the gold nanorods coated with a mesoporous silica layer were created via the Ye & Murray's method. These rods have an aspect ratio between 2 and 3. As mentioned before, the aspect ratio of the gold nanorods should be more in the order of 8 or 9 to achieve the desirable particles. So using the Chang & Murphy's method, high aspect ratio gold nanorods were synthesized, as discussed in chapter 2. In the following experiments, these high AR gold nanorods were coated with mesoporous silica. Here Au-NR010 was chosen (AR of 8.3, for size see table 2).

In the synthesis, TEOS is dissolved in MeOH to slow down the reaction. As it isn't yet clear at which time the PEG-Silane should be added - the higher aspect ratio rods have less surface and the gold concentration isn't the same as with the previous synthesis - 6 batches of gold nanorods were coated with silica where the PEG-Silane was added at different times (10, 20, 30, 45 and 60 min and one batch were no PEG-Silane was added as reference). It was chosen to add more PEG in the earlier time scale (thus before 30 minutes) as the results of figure 3.3 show that the thickness of silica after 30 minutes is already around 12 nm.

Synthesis

In six 40 mL vials 7.0 mL water, 1.0 mL CTAB (5 mM) and 2.0 mL of batch Au-NR010 (gold concentration of around $1.1*10^{13}$ mL^{-1}) was added. The vials were placed in a water bath of 30 °C while stirring at 400 rpm. After about 5 min 100 µL NaOH (0.1 M) was added. A 20% TEOS-solutions were made, by dissolving 200 µL TEOS in 800 µL MeOH (100%). In eight vials 30 µL TEOS solution was added. At different time intervals (10, 20, 30, 45 and 60 min) 40 µL PEG-Silane was added. In one vial no PEG-Silane was added.

After two days the samples were washed one time with water and two times with EtOH (96%). Centrifuged in 15 mL falcon tubes for 15 min at 8000 rcf at 23 °C. Each time the supernatant was discarded and the sediment was redispersed. The sediments were sonicated and vortexed for a few seconds. In the end, the samples were dissolved in 1.0 mL EtOH (100%). All silica-coated gold nanorod samples were stored in the fridge for stability. The thickness of the silica layers was investigated with the use of TEM.

Results

Figure 3.6 shows the TEM images of each of the six samples. Figure 3.5 shows the thicknesses of the silica layers against the time when PEG-Silane is added and the aspect ratios of the silica-coated gold

nanorods against the time PEG-Silane is added. Table 6 listed the thicknesses of the silica layers for the different batches. Adding the PEG-Silane after 10 minutes doesn't result in the formation of a silica layer. Apparently, the PEG-Silane is added too soon, so no stable silica layer is formed. This is in agreement with the literature [76]. After 20 minutes a stable silica layer is formed. Unfortunately, the silica layer is slightly too thick, resulting in an aspect ratio of 3.97. This is slightly below the aimed aspect ratio of 4.5. But more concerning is the rough layer. The layer would probably be too rough to give good self-assembly. This is probably because the PEG-silane was, for this sample, added at 20 min. The TEOS does not have much time to form a smooth layer. Even for the batch at 45 min, the silica layer looks rough. Rougher than for example the batch from 45 min of the EtOH/MeOH experiment. This can probably be attributed to the lower concentration of gold nanorods (2 mL of $1.1*10^{13}$ mL^{-1} gold

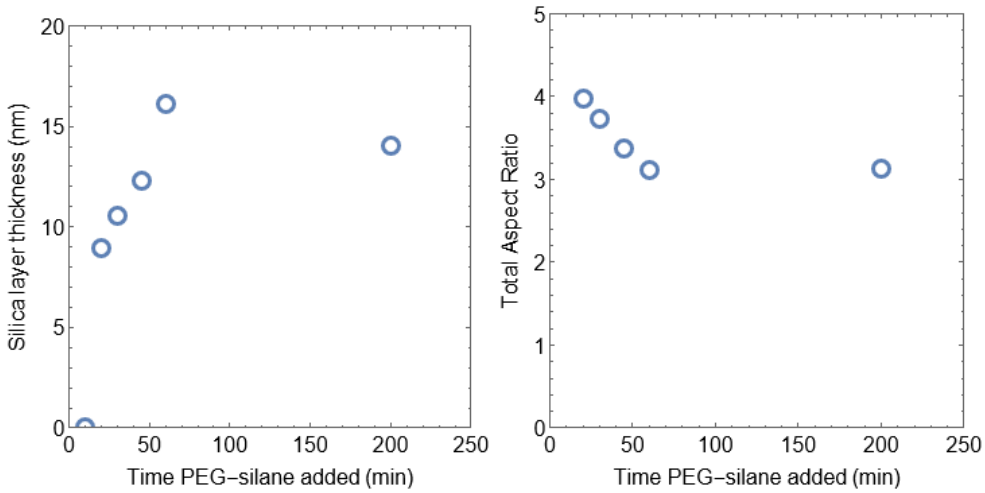

(a) (b)

Figure 3.5: The silica layer thickness (a) and total aspect ratio of the silica-coated gold nanorods (b) compared to the time PEG-Silane was added. The sample where no PEG-Silane was added is set at t=200 min. The precise lengths can be found in table 6. TEM images can be found in figure 3.6. The aspect ratio of the uncoated Au NR is 8.43.

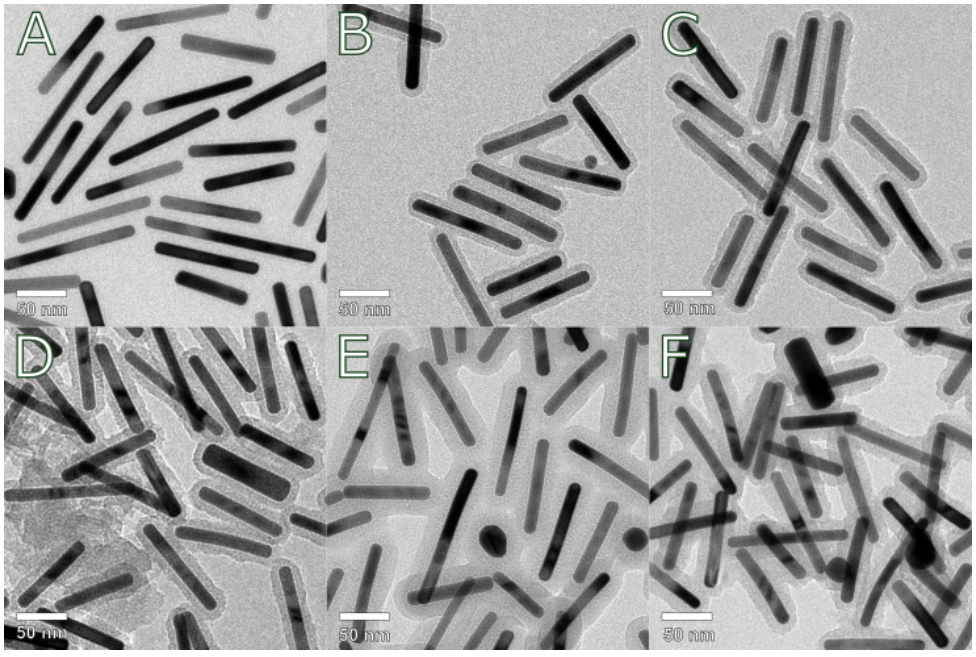

Figure 3.6: TEM images of the silica-coated Au-NR010 (AR of 8.4, $1.1*10^{13}$ particles per mL). PEG-Silane was added at 10, 20, 30, 45 and 60 min (A till E respectively.). In F no PEG-Silane was added. The thickness of the silica layers can be found in table 6.

nanorods added instead of $6.38*10^{12}$ mL^{-1} in the previous experiment).

3.6 Silica-coated high aspect ratio gold nanorods with high concentration gold nanorods

As the concentration of the gold nanorods might influence the formation of smooth silica layers, the experiment was repeated with a higher gold nanorod concentration. As there isn't an infinite supply of these high aspect ratio gold nanorods, the scale of the coating was put back from 10 mL to a 2.5 mL. This should not influence the silica layer that is formed, but saves a bit on the rods needed. Still, two batches of gold are used, as just using one doesn't provide enough rods.

Gold batches Au-NR012A (AR of 8.25) and Au-NR012C (AR of 9.16) were used, for sizes see table 1. PEG-Silane was added at 15, 30 and 45 min and in one batch no PEG-Silane was added. These times were chosen based on the previous results.

Synthesis

In 8 mL vials 1.25 mL water, 250 µL CTAB (5 mM) and 500 µL Au-NR012A ($4.60*10^{12}$ mL^{-1}) or Au-NR012C ($3.80*10^{12}$ mL^{-1}) was added. The vials were placed in a water bath of 30 °C while stirring at 400 rpm. After about 5 min 100 µL NaOH (0.1 M) was added. A 20% TEOS solutions were made, by dissolving 400 µL TEOS in 1.6 mL MeOH (100%). In the six vials 15 µL TEOS solution was added. At different time intervals (30, 45 and 60 min) 20 µL PEG-Silane was added to three of the vials. In one vial no PEG-Silane was added. For the samples where PEG-Silane was added after 15 and 30 min Au-NR012A was used and for the samples where PEG-Silane was added after 60 min and no PEG-Silane was added Au-NR012C was used.

After two days, the samples were washed one time with water and two times with EtOH (96%). Centrifuged in 15 mL falcon tubes for 15 min at 8000 RCF at 23 °C. Each time the supernatant was discarded and the sediment was redispersed. The sediments were sonicated and vortexed for a few seconds. In the end, the samples were dissolved in 1.0 mL EtOH (100%). All silica-coated gold nanorod samples were stored in the fridge for stability. The thickness of the silica layers was investigated with the use of TEM.

Results

Figure 3.7 shows the TEM images of the four samples. The batch with no PEG-Silane (figure 3.7D) shows a smooth silica layer. The thickness is slightly thicker than the sample where no PEG-silane was added in the previous experiment. It is, however, more monodisperse; 15.3 nm (±1.21 nm) compared to 14.07 (±2.08). It could be that the higher concentration of gold yields a more controlled growth, resulting in more similar silica thickness. It is also possible that this is due to the lower scale.

For the samples without PEG-Silane, no silica layer was formed. This is not as expected as without PEG-Silane a thick smooth layer should form, as can be seen in various results throughout this chapter. It is unclear why in this experiment no silica layer is formed. It could be that due to the higher concentration of gold nanorods, the formation of the silica layer goes a bit slower. If this is the case, then no stable silica layer was formed before the PEG-Silane was added. This could also explain why the silica layer that was formed without added PEG-Silane is more smooth than in the previous experiment; when the

Time PEG added (min)	Silica layer thickness (nm)	Total Aspect Ratio
10	0	8.43 (±2.81)
20	8.92 (±1.89)	3.97 (±0.77)
30	10.54 (±1.69)	3.73 (±0.72)
45	12.33 (±1.69)	3.37 (±0.62)
60	16.13 (±2.68)	3.12 (±0.72)
No PEG	14.07 (±2.08)	3.13 (±0.66)

Table 6: The thickness of the silica layer and the aspect ratio of the coated Au-NR010 (gold concentration of $1.1*10^{13}$ mL^{-1}, AR of 8.43) with PEG-Silane added at different time intervals. The experiment was done in 5 mL-scale, 30 µL of TEOS (20%) added, while the TEOS was dissolved in MeOH, 40 µL PEG-Silane added to each vial.

growth is slow it will become more smooth. This would also explain why the standard deviation of the silica layer is smaller than in the previous experiment.

It would have been nice to repeat this experiment but add the PEG-Silane at a later time to see if this would yield a stable silica shell. Unfortunately, due to the problems with the gold nanorod formation, no high aspect ratio rods were left to perform this experiment.

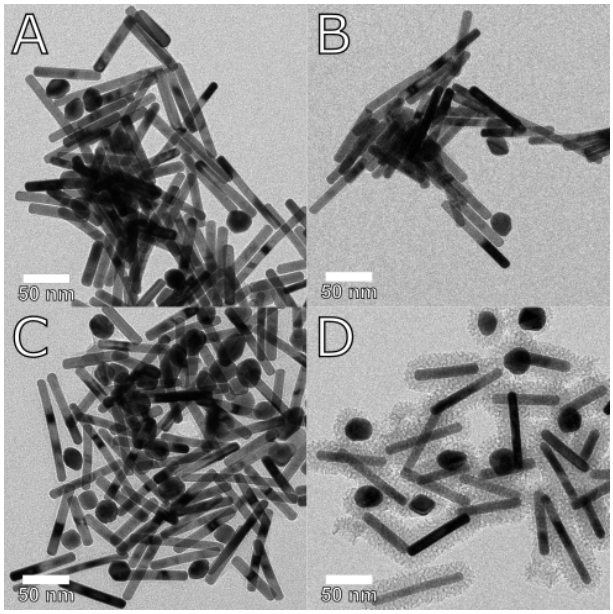

Figure 3.7: The TEM images of the coated Au-NR012 (A and B) and Au-NR014 (C and D). PEG-Silane is added at 15 min (A), 30 min (B), 45 min (C) and not added at all (D). In the batches, A-C is no silica layer formed at all. In batch D a silica layer of 15.3 nm ($\pm$1.21 nm) is formed.

4 Conclusions

The goal of the research was to create the best colloidal system for Surface Enhance Raman Spectroscopy. It is shown that the use of silica-coated gold nanorods would be a good candidate for this colloidal system. Gold itself provides a strong electromagnetic enhancement without it being toxic. Further, the strong curvature of the tips of the rods will result in an even stronger enhancement. If the gold nanorods could be aligned in an end-to-end configuration, then plasmonic hotspots can be formed where the electromagnetic field is even stronger leading to the highest enhancement. The creation of a smectic ordered liquid crystal - here the rods are oriented towards the same direction and layer by layer - would be a novel way to create the end-to-end configuration without the need for further surface modifications. To gain smectic ordering, the aspect ratio of the nanoparticle should be higher than 4.1.

The gold nanorods were coated in mesoporous silica oxide as this would improve thermal stability and reduce toxicity. The mesoporous holes allow for further chemical treatment of the gold nanorod. Further, the silica layer will shield the strong van der Waals interaction of the gold nanorods. The silica coating has to have a certain thickness to prevent aggregation of the nanorods, however, the thicker the silica layer, the lower the aspect ratio of the particle. Because of this, the gold nanorod should have a high enough aspect ratio to allow the silica layer to be thick enough to prevent aggregation, while the total aspect ratio is still above 4.1. It was calculated that the aspect ratio of the gold nanorod should be at least 6.9.

In this thesis, gold nanorods were achieved with various aspect ratios ranging from 2.2 to 5.6 via the Ye & Murray's method. Using the Chang & Murphy's method gold nanorods with an aspect ratio up to 8.5 could be synthesized. Over time, however, it seems impossible to gain such a high aspect ratio due to a bottle of $NaBH_4$ becoming too old or bad NaOH stock solutions. Ordering a new bottle of $NaBH_4$ didn't fix the problem due to the impurities in the bottle.

Several batches of gold nanorods were coated with a silica layer. Changing the concentration of TEOS, wasn't a good way to gain control over the thickness of the silica layer. However, adding PEG-silane to the reaction at different time intervals was a good way to create silica-coated gold nanorods with a certain silica thickness. Dissolving the silica precursor TEOS in methanol instead of ethanol slows down the speed at which the silica layer is formed. This allows for even further control over the silica layer. However, gaining full control over the thickness of the silica layer is still difficult as it also depends on the concentration and the dimensions of the gold nanorods.

In the end, the best batch of silica-coated gold nanorods had a gold aspect ratio of 8.11 and a total aspect ratio of 3.98. However, not only was the silica layer slightly too thick, but the layer itself was also rough. This could cause problems with self-assembly.

For the future, it is a good idea to investigate if using a new bottle of $NaBH_4$ of the same supplier as before fixes the problem. Further, it is worth looking into how the concentration and the dimensions of the gold nanorods influence the growth rate of the silica layer. This would allow for a better estimation of when the PEG-silane should be added to gain the desired thickness.

5 Acknowledgements

Science is never done alone. Therefore I would like to thank a few people who helped me during my master's thesis. First of all, I would like to thank my first supervisor Alfons. First of all for allowing me the opportunity to do my master's thesis at the SCM lab. I learned a lot about gold and colloidal systems. Second, I would like to thank him for his input and knowledge about the subject. Further, I would like to thank my second supervisor Arnout for his input. The last supervisor I would like to thank is of course my daily supervisor Harith. Without his help explaining the syntheses, showing me around the lab and being there if I had questions, this thesis would never have been a success.

Other people that I would like to thank are everybody from the *informal experimental meeting* for listening to my problems and thinking along in solving the problems. I would also like to thank the SCM group as a whole for their open atmosphere during their lunches and in the lab. I felt very welcome. Also, a thank you towards the students in the student room for their companionship and for listening to me complaining about my gold nanorod synthesis failing over and over again. I would especially thank Geert, Jeffery, René, and Dinja for their help with Latex and Mathematica.

At last I would like to thank my mother Anja and my brother Marc Paul for proofreading and spelling-checking my thesis.

A Appendix

A.1 General synthesis steps

Cleaning the glassware

As the gold nanorod formation can be very sensitive to small impurities in the glassware, it is really important that the glassware used is as clean as possible. For this reason, all the glassware and stirring bars used, except for the one-use glassware, were cleaned with aqua regia. All aqua regia was freshly made by mixing hydrochloric acid (37% v/v) with nitric acid in a 3:1 volume ratio. After 12 h the aqua regia was rinsed away with large amounts of water and then dried at 100 °C for 24 h. The one-use glassware (all the falcon tubes, Eppendorf tubes and 40 mL vials) were not cleaned as they were used as purchased.

Preparing TEM samples

To prepare the gold nanorod samples for the TEM, the CTAB needs to be (partially) washed away to better see the gold nanorods. As the gold nanorods could easily aggregate when the CTAB is partially washed away, the samples need to be diluted. All TEM samples were prepared in the following way: 100 µL of the gold nanorod samples were diluted in 200 µL water in 500 µL eppendorf tubes. These tubes were centrifuged for 5 min at 8000 rcf. The supernatant was discarded and the sediment redispersed in 200 µL water. 10 µL was dropcasted onto the TEM grid and dried overnight.

To prepare the silica-coated gold nanorods samples for the TEM the following procedure was followed: 100 µL sample was dissolved in 100 µL EtOH (100%). 10 µL was put onto the TEM grid and dried for a few minutes.

A.2 Extra figures

Figure A.1: The Lycurgus cup, a cup from the fourth century, made by the Romans uses gold and silver nanoparticles. The cup shows two colours depending on where the light comes from. The green colour is because of scattering; the one on the right is due to absorbance.

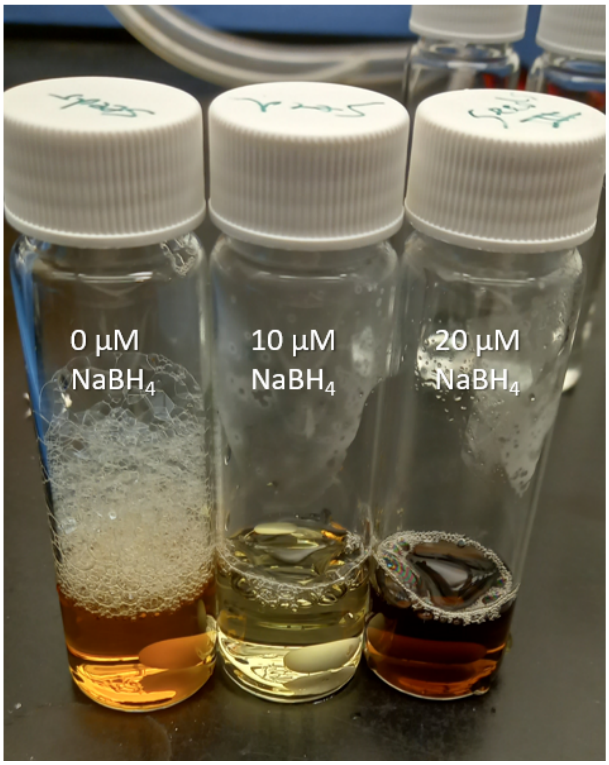

Figure A.2: A photo of three different seed solutions. The one on the left is the seed solution just before the addition of $NaBH_4$, the one in the middle has 10 µM $NaBH_4$ added and the one on the left has 20 µM $NaBH_4$ added.

B Chemicals and Apparatus used

Chemical used

The following chemicals were used in the experiments: Ethanol (EtOH 100%, Interchema no. I-AS.102.46D), Ethanol (EtOH 95%, VWR Chemicals no. 64-17-5), Hexadecyltrimethylammonium bromide (CTAB, >98%, TCL no. H0081), Hydrochloric acid (HCl 37% aqueous solution, Sigma-Aldrich no. 258148), Hydrogen tetrachloroaurate trihydrate ($HAuCl_4(H_2O)_3$ Sigma-Aldrich >99.9%,), Hydroquinone (>99% Fluka no. 53960), L-Ascorbic acid (AA, >99%, Sigma-Aldrich noA5960), Methanol (MeOH 100%, prac., Interchema no. 603-001-00-X). Nitric acid (HNO_3, 65% aqueous solution, Acros Organics no. 124660025), 2-(Methoxy(polyethyleneoxy)propyl)trimethoxysilane (PEG-Silane), Silver nitrate ($AgNO_3$,>99.0%, Sigma-Aldrich no. 209139), Sodium borohydride ($NaBH_4$, >99% no.213462), Sodium borohydride ($NaBH_4$, >98.0% no.452882, only used in the last synthesis) Sodium hydroxide (NaOH, Acros Organics no. 134070010), Sodium Oleate (NaOL, >97% TLC no. O0057), Tetraethyl orthosilicate (TEOS, 98% Sigma-Aldrich no. 376213) Further Ultrapure water (Millipore Milli-Q grade) with a resistivity of 18.2 MΩ was used in all of the experiment

Apparatus used

The following centrifuges were used:

- Eppendorf 5415C with an F-45-18-11 fixed angle rotor for 2 mL Eppendorf tubes
- Eppendorf 5424R with an FA-45-24-11 fixed angle rotor for 2 mL Eppendorf tubes
- Eppendorf 5430R with an FA-45-24-11 fixed angle rotor for 5 mL Eppendorf tubes
- Hettich Rotina 380R with a 1720 fixed angle rotor for 15 mL and 40 mL centrifuge tubes

For the TEM images the FEI Talos L120C was used. The absorption spectra were recorded with the Bruker Verter 70 FT-IR with a quartz beamsplitter and a Si diode detector.

C Calculations

In the book "Van der Waals forces: a handbook for biologists, chemists, engineers, and physicists" of 2006, Parsegian [40] gives two equations for the calculation of van der Waals interactions for rod-shaped particles: one in the *far regime*, where the distance between the rods is much bigger than the radius, and one in the *close regime*, where the distance between the rods is much smaller than the radius. As discussed in the introduction, it is useful to rewrite these equations in terms of aspect ratio to estimate the minimal aspect ratio the gold rods should have for it to be coated with a thick enough silica layer to prevent aggregation, while the total aspect ratio is still above 4.1.

Parsegian also gives a more general equation, which can be used in both regimes. It can also be used in the case where the distance between the rods is around the same size as the thickness of the rods. This would be the better equation to use here, as this is likely the case. However, since this generalised equation contains a gamma function, it is impossible to rewrite this equation in terms of aspect ratios. In the introduction, only the cylinder far regime is mentioned even though this isn't entirely correct. The justification for only using this regime is that the calculation in the close regime actually gives an answer that would be in the far regime. Namely, the gold rod should have an aspect ratio of 64.2 while the silica-coated gold rod would still have an aspect ratio of 4.1.

C.1 Cylinders far regime

Parsegian gives for the far regime the following equation:

$$U_{vdW}(z) = -\frac{3}{8\pi} A_H \frac{(\pi R^2)^2 L}{z^5} \tag{C.1}$$

with 'U_{vdW}' the van der Waals potential between two rods separated by distance 'z', A_H is the Hamaker constant, R is the radius of the gold rod, L is the length of the gold rod and z is the distance between the two gold rods (see also figure 1.10). Since we are looking at how big the attraction is between two particles which are only separated by their own radius and the silica thickness (h), so the distance 'z' becomes 2R+2h.

$$U_{vdW}(2R + 2H) = -\frac{3}{8\pi} A_H \frac{(\pi R^2)^2 L}{(2R + 2h)^5} \tag{C.2}$$

In the introduction, two definitions of aspect ratios are formulated (C.3 and C.4), which are the aspect ratio of the gold nanorod and the aspect ratio of the silica-coated gold nanorod:

$$\Gamma_G = \frac{L}{W} = \frac{L}{2R} \tag{C.3}$$

$$\Gamma_T = \frac{L + 2h}{2R + 2h} \tag{C.4}$$

To get an expression of 'U_{vdW}' in units of 'Γ_G' and 'Γ_T', the units 'L', 'R' and 'h' needs to be replaced by these two terms eventually.

Using $\Gamma_G = \frac{L}{2R}$ and thus $R = \frac{L}{2\Gamma_G}$ we could rewrite C.2 to

$$U_{vdW} = -\frac{3}{8\pi} A_H \frac{(\pi(\frac{L}{2\Gamma_G})^2)^2 L}{(2\frac{L}{2\Gamma_G} + 2h)^5} \tag{C.5}$$

$$U_{vdW} = -\frac{3\pi}{128} A_H \frac{L^5 \Gamma_G}{(L + 2\Gamma_G h)^5} \tag{C.6}$$

In equation C.6, we got rid of the 'R' term, but we're still left with 'L' and 'h'. Also, Γ_T needs to be introduced. One way of doing this is by defining 'h' as a function of 'Γ_T'. To do that equation C.4 needs to be rewritten to:

$$\Gamma_T = \frac{L + 2h}{2R + 2h} \tag{C.7}$$

$$h = \frac{L - 2\Gamma_T R}{2\Gamma_T - 2} \tag{C.8}$$

Substitution this definition of h into the equation C.6 leads to:

$$U_{vdW} = -\frac{3\pi}{128} A_H \frac{L^5 \Gamma_G}{\left(L + 2\Gamma_G \left(\frac{L - 2\Gamma_T R}{2\Gamma_T - 2}\right)\right)^5} \tag{C.9}$$

$$U_{vdW} = -\frac{3\pi}{128} A_H \frac{L^5 \Gamma_G (\Gamma_T - 1)^5}{(\Gamma_T L - L + \Gamma_G L - 2\Gamma_G \Gamma_T R)^5} \tag{C.10}$$

Again using $R = \frac{L}{2\Gamma_G}$ we get

$$U_{vdW} = -\frac{3\pi}{128} A_H \frac{L^5 \Gamma_G (\Gamma_T - 1)^5}{\left(\Gamma_T L - L + \Gamma_G L - 2\Gamma_G \Gamma_T \left(\frac{L}{2\Gamma_G}\right)\right)^5} \tag{C.11}$$

$$U_{vdW} = -\frac{3\pi}{128} A_H \Gamma_G \left(\frac{\Gamma_T - 1}{\Gamma_G - 1}\right)^5 \tag{C.12}$$

Which is an expression for U_{vdW} which is solely based on both expressions of aspect ratios. This is the expression given in the introduction (equation 1.13).

For the calculation in the introduction, we want U_{vdW} not to be lower than a certain value (such as -1.5 K_bT). We can use this value to calculate the minimum value of Γ_G and Γ_T, by rewriting this equation as a definition of Γ_G:

$$U_{vdW} \leq \frac{3\pi}{128} A_H \frac{\Gamma_G (\Gamma_T - 1)^5}{(\Gamma_G - 1)^5} \tag{C.13}$$

$$\Gamma_G^{\frac{4}{5}} - \Gamma_G^{-\frac{1}{5}} \geq (\Gamma_T - 1) \sqrt[5]{\frac{3\pi A_H}{128 U_{vdW}}} \tag{C.14}$$

Unfortunately, it seems that we cannot isolate Γ_G any further. According to the Abel-Ruffini theorem, it is impossible to solve a polynomial equation of fifth degree or higher with arbitrary coefficients [80]. However, because there is only one term of Γ_T in equation C.12, Γ_T can be isolated.

$$U_{vdW} \leq -\frac{3\pi}{128} A_H \frac{\Gamma_G (\Gamma_T - 1)^5}{(\Gamma_G - 1)^5} \tag{C.15}$$

$$\Gamma_T \geq 1 + (\Gamma_G - 1) \sqrt[5]{\frac{3\pi A_H \Gamma_G}{128 U_{vdW}}} \tag{C.16}$$

Using analytical tools, this equation can be used to calculate what the minimum value of Γ_G should be. If we take 73 K_BT for the value of A_H and 1.5 K_BT for U_{vdW} and want Γ_T not to be lower than 4.1, then the value of Γ_G should then be 6.9. This is the value that is discussed in the introduction.

C.2 Cylinders close regime

As mentioned earlier, the book of Parsegian gives another equation for calculating the Vanderwaals potential; the one in the so called close regime, where the distance between the rods is much smaller than the radius of the rods. Here similar things can be done to calculate what the aspect ratio of the gold rod should be.

Parsegian gives for the close regime the following equation:

$$U_{Vdw}(z) = -\frac{A_h}{24}\frac{LR^{\frac{1}{2}}}{z^{\frac{3}{2}}} \tag{C.17}$$

Which, when the particles are right next to each other becomes:

$$U_{Vdw}(2R+2h) = -\frac{A_h}{24}\frac{LR^{\frac{1}{2}}}{(2R+2h)^{\frac{3}{2}}} \tag{C.18}$$

Using $R = \frac{L}{2\Gamma_G}$ the equation becomes:

$$U_{vdW} = -\frac{A_h}{24}\frac{L\left(\frac{L}{2\Gamma_G}\right)^{\frac{1}{2}}}{\left(2\left(\frac{L}{2\Gamma_G}\right)+2h\right)^{\frac{3}{2}}} \tag{C.19}$$

$$U_{vdW} = -\frac{A_h}{24\sqrt{2}}\frac{\Gamma_G L^{\frac{3}{2}}}{(L+2h\Gamma_G)^{\frac{3}{2}}} \tag{C.20}$$

$$\tag{C.21}$$

Using $h = \frac{L-2\Gamma_T R}{2\Gamma_T - 2}$ gives:

$$U_{vdW} = -\frac{A_h}{24\sqrt{2}}\frac{\Gamma_G L^{\frac{3}{2}}}{\left(L+2\left(\frac{L-2\Gamma_T R}{2\Gamma_T-2}\right)\Gamma_G\right)^{\frac{3}{2}}} \tag{C.22}$$

$$U_{vdW} = -\frac{A_h}{24\sqrt{2}}\frac{\Gamma_G L^{\frac{3}{2}}(\Gamma_T-1)^{\frac{3}{2}}}{(L\Gamma_T - L + L\Gamma_G - 2\Gamma_T R\Gamma_G)^{\frac{3}{2}}} \tag{C.23}$$

$$\tag{C.24}$$

Again using $R = \frac{L}{2\Gamma_G}$ gives:

$$U_{vdW} = -\frac{A_h}{24\sqrt{2}}\frac{\Gamma_G L^{\frac{3}{2}}(\Gamma_T-1)^{\frac{3}{2}}}{(L\Gamma_T - L + L\Gamma_G - 2\Gamma_T\left(\frac{L}{2\Gamma_G}\right)\Gamma_G)^{\frac{3}{2}}} \tag{C.25}$$

$$U_{vdW} = -\frac{A_h\Gamma_G}{24\sqrt{2}}\left(\frac{\Gamma_T-1}{\Gamma_G-1}\right)^{\frac{3}{2}} \tag{C.26}$$

Also here the minimal aspect ratio for the gold can be calculated:

$$U_{vdW} \leq -\frac{A_h\Gamma_G}{24\sqrt{2}}\frac{(\Gamma_T-1)^{\frac{3}{2}}}{(\Gamma_G-1)^{\frac{3}{2}}} \tag{C.27}$$

$$\Gamma_T \geq 1 + (\Gamma_G - 1)\left(\frac{24\sqrt{2}U_{vdW}}{A_h\Gamma_G}\right)^{\frac{2}{3}} \tag{C.28}$$

Using analytics tools, this equation can be used to calculate which value Γ_G should have for Γ_T to not exceed 4.1 (using 1.5 K_BT for U_{vdW} and 73 K_BT for A_H). This value is 64.2. This value is bigger than the value when the far regime calculation is used. However, as the gold nanorod needs to have an aspect ratio of 64.2 and the silica-coated gold rod has an aspect ratio of 4.1, then the silica layer will be very thick. This means that the distance between the two rods is much more than the radius of the rod, thus that we no longer can use the close regime calculation. For this reason, it was chosen to use the far regime calculation in the introduction.

D References

[1] E. C. Le Ru and P. G. Etchegoin, *Principles of Surface-Enhanced Raman Spectroscopy*. Amsterdam: Elsevier B.V., first ed., 2009.

[2] P. Kim, W. Xiong, and R. E. Continetti, "Evolution of Hydrogen-Bond Interactions within Single Levitated Metastable Aerosols Studied by in Situ Raman Spectroscopy," *J. Phys. Chem. B*, vol. 124, no. 42, pp. 9385–9395, 2020.

[3] M. Rudolph and U. A. Peuker, "Mapping hydrophobicity combining AFM and Raman spectroscopy," *Miner. Eng.*, vol. 66, pp. 181–190, 2014.

[4] J. Zheng and L. He, "Surface-Enhanced Raman Spectroscopy for the Chemical Analysis of Food," *Compr. Rev. Food Sci. Food Saf.*, vol. 13, pp. 317–328, may 2014.

[5] P. Vandenabeele and H. Edwards, eds., *Raman Spectroscopy in Archaeology and Art History Volume 2*. Croydon: Royal Society of Chemistry, first ed., 2019.

[6] P. Vandenabeele, H. G. M. Edwards, and J. Jehlička, "The role of mobile instrumentation in novel applications of Raman spectroscopy: archaeometry, geosciences, and forensics," *Chem. Soc. Rev.*, vol. 43, no. 8, p. 2628, 2014.

[7] C. Kallaway, L. M. Almond, H. Barr, J. Wood, J. Hutchings, C. Kendall, and N. Stone, "Advances in the clinical application of Raman spectroscopy for cancer diagnostics.," *Photodiagnosis Photodyn. Ther.*, vol. 10, pp. 207–19, sep 2013.

[8] X. Wang, S. C. Huang, S. Hu, S. Yan, and B. Ren, "Fundamental understanding and applications of plasmon-enhanced Raman spectroscopy," *Nat. Rev. Phys.*, vol. 2, no. 5, pp. 253–271, 2020.

[9] J. R. Ferraro, K. Nakamoto, and C. W. Brown, *Introductory Raman Spectroscopy*. Orlando: Academic Press, second ed., 2003.

[10] P. Matousek, M. Towrie, and A. W. Parker, "Fluorescence background suppression in Raman spectroscopy using combined Kerr gated and shifted excitation Raman difference techniques," *J. Raman Spectrosc.*, vol. 33, pp. 238–242, apr 2002.

[11] P. Bharadwaj, B. Deutsch, and L. Novotny, "Optical Antennas," *Adv. Opt. Photonics*, vol. 1, p. 438, nov 2009.

[12] M. Prochazka, *Surface-Enhanced Raman Spectroscopy*. Biological and Medical Physics, Biomedical Engineering, Cham: Springer International Publishing, first ed., 2016.

[13] E. V. Anslyn, D. A. Dougherty, and J. Murdzek, *Modern Physical Organic Chemistry*. Sausalito: University Science Books, 2006 ed., 1960.

[14] P. K. Jain and M. A. El-Sayed, "Plasmonic coupling in noble metal nanostructures," *Chem. Phys. Lett.*, vol. 487, pp. 153–164, mar 2010.

[15] S.-Y. Ding, E.-M. You, Z.-Q. Tian, and M. Moskovits, "Electromagnetic theories of surface-enhanced Raman spectroscopy," *Chem. Soc. Rev.*, vol. 46, no. 13, pp. 4042–4076, 2017.

[16] S. Eustis and M. A. El-Sayed, "Why gold nanoparticles are more precious than pretty gold: noble metal surface plasmon resonance and its enhancement of the radiative and nonradiative properties of nanocrystals of different shapes.," *Chem. Soc. Rev.*, vol. 35, pp. 209–17, mar 2006.

[17] H.-H. Chang and C. J. Murphy, "Mini Gold Nanorods with Tunable Plasmonic Peaks beyond 1000 nm," *Chem. Mater.*, vol. 30, pp. 1427–1435, feb 2018.

[18] "Surface Plasmon." `https:en.wikipedia.org/wiki/Surface_plasmon`. Accessed: 01-12-2022.

[19] K. L. Kelly, E. Coronado, L. L. Zhao, and G. C. Schatz, "The Optical Properties of Metal Nanoparticles: The Influence of Size, Shape, and Dielectric Environment," *J. Phys. Chem. B*, vol. 107, pp. 668–677, jan 2003.

[20] M. Faraday, "Experimental Relations o f Gold (and other Metals) to Light.," *Phil. Trans. R. Soc.*, vol. 147, no. 0, pp. 145–181, 1857.

[21] G. Mie, "Beiträge zur Optik trüber Medien, speziell kolloidaler Metallösungen," *Ann. Phys.*, vol. 330, no. 3, pp. 377–445, 1908.

[22] C. Zong, M. Xu, L.-J. Xu, T. Wei, X. Ma, X.-S. Zheng, R. Hu, and B. Ren, "Surface-Enhanced Raman Spectroscopy for Bioanalysis: Reliability and Challenges," *Chem. Rev.*, vol. 118, pp. 4946–4980, may 2018.

[23] Y. Cao, J. Zhang, Y. Yang, Z. Huang, N. V. Long, and C. Fu, "Engineering of SERS substrates based on noble metal nanomaterials for chemical and biomedical applications," *Appl. Spectrosc. Rev.*, vol. 50, pp. 499–525, jul 2015.

[24] S. Link, M. A. El-Sayed, and B. Mohamed, "Simulation of the Optical Absorption Spectra of Gold Nanorods as a Function of Their Aspect Ratio and the Effect of the Medium Dielectric Constant," *J. Phys. Chem. B*, vol. 109, pp. 10531–10532, may 1999.

[25] P. G. Etchegoin and E. C. Le Ru, "A perspective on single molecule SERS: current status and future challenges," *Phys. Chem. Chem. Phys.*, vol. 10, no. 40, p. 6079, 2008.

[26] H. Xu, E. J. Bjerneld, J. Aizpurua, P. Apell, L. Gunnarsson, S. Petronis, B. Kasemo, C. Larsson, F. Hook, and M. Kall, "Interparticle coupling effects in surface-enhanced Raman scattering," *Proc. SPIE*, vol. 4258, pp. 35–42, 2001.

[27] S. L. Kleinman, R. R. Frontiera, A. I. Henry, J. A. Dieringer, and R. P. Van Duyne, "Creating, characterizing, and controlling chemistry with SERS hot spots," *Phys. Chem. Chem. Phys.*, vol. 15, no. 1, pp. 21–36, 2013.

[28] R. C. Maher and C. S. S. R. Kumar, *Raman Spectroscopy for Nanomaterials Characterization*, vol. 9783642206. Berlin, Heidelberg: Springer Berlin Heidelberg, 2012.

[29] M. G. Blaber, M. D. Arnold, and M. J. Ford, "A review of the optical properties of alloys and intermetallics for plasmonics," *J. Phys. Condens. Matter*, vol. 22, no. 14, 2010.

[30] J. M. Sanz, D. Ortiz, R. Alcaraz De La Osa, J. M. Saiz, F. González, A. S. Brown, M. Losurdo, H. O. Everitt, and F. Moreno, "UV plasmonic behavior of various metal nanoparticles in the near- and far-field regimes: Geometry and substrate effects," *J. Phys. Chem. C*, vol. 117, no. 38, pp. 19606–19615, 2013.

[31] D. M. Solís, J. M. Taboada, F. Obelleiro, L. M. Liz-Marzán, and F. J. García de Abajo, "Optimization of Nanoparticle-Based SERS Substrates through Large-Scale Realistic Simulations," *ACS Photonics*, vol. 4, pp. 329–337, feb 2017.

[32] C. Hamon, S. M. Novikov, L. Scarabelli, D. M. Solís, T. Altantzis, S. Bals, J. M. Taboada, F. Obelleiro, and L. M. Liz-Marzán, "Collective Plasmonic Properties in Few-Layer Gold Nanorod Supercrystals," *ACS Photonics*, vol. 2, pp. 1482–1488, oct 2015.

[33] L. Vigderman, B. P. Khanal, and E. R. Zubarev, "Functional Gold Nanorods: Synthesis, Self-Assembly, and Sensing Applications," *Adv. Mater.*, vol. 24, pp. 4811–4841, sep 2012.

[34] G. Kawamura, Y. Yang, and M. Nogami, "Facile assembling of gold nanorods with large aspect ratio and their surface-enhanced Raman scattering properties," *Appl. Phys. Lett.*, vol. 90, p. 261908, jun 2007.

[35] P. Bolhuis and D. Frenkel, "Tracing the phase boundaries of hard spherocylinders," *J. Chem. Phys.*, vol. 106, pp. 666–687, jan 1997.

[36] M. A. Boles, M. Engel, and D. V. Talapin, "Self-Assembly of Colloidal Nanocrystals: From Intricate Structures to Functional Materials," *Chem. Rev.*, vol. 116, pp. 11220–11289, sep 2016.

[37] M. A. Bates and D. Frenkel, "Influence of polydispersity on the phase behavior of colloidal liquid crystals: A Monte Carlo simulation study," *J. Chem. Phys.*, vol. 109, pp. 6193–6199, oct 1998.

[38] J. F. Li, Y. F. Huang, Y. Ding, Z. L. Yang, S. B. Li, X. S. Zhou, F. R. Fan, W. Zhang, Z. Y. Zhou, D. Y. Wu, B. Ren, Z. L. Wang, and Z. Q. Tian, "Shell-isolated nanoparticle-enhanced Raman spectroscopy," *Nature*, vol. 464, pp. 392–395, mar 2010.

[39] J. E. S. Van Der Hoeven, *Gold based Nanorods Tuning the Structure for Catalysis and Sensing.* Utrecht: Proefschitftmaken.nl, 1 ed., 2019.

[40] V. A. V. A. Parsegian, *Van der Waals forces : a handbook for biologists, chemists, engineers, and physicists*. Cambridge: Cambridge University Press, first ed., 2006.

[41] T. H. Anderson, Y. Min, K. L. Weirich, H. Zeng, D. Fygenson, and J. N. Israelachvili, "Formation of Supported Bilayers on Silica Substrates," *Langmuir*, vol. 25, pp. 6997–7005, jun 2009.

[42] S. J. Blundell and K. M. Blundell, *Concepts in Thermal Physics*. Oxford: Oxford University Press, 2nd ed., oct 2009.

[43] J. H. Yoon, F. Selbach, L. Langolf, and S. Schlücker, "Ideal Dimers of Gold Nanospheres for Precision Plasmonics: Synthesis and Characterization at the Single-Particle Level for Identification of Higher Order Modes," *Small*, vol. 14, no. 4, pp. 1–5, 2018.

[44] X. Ye, C. Zheng, J. Chen, Y. Gao, and C. B. Murray, "Using Binary Surfactant Mixtures To Simultaneously Improve the Dimensional Tunability and Monodispersity in the Seeded Growth of Gold Nanorods," *Nano Lett.*, vol. 13, pp. 765–771, feb 2013.

[45] C. J. Huang, Y. H. Wang, P. H. Chiu, M. C. Shih, and T. H. Meen, "Electrochemical synthesis of gold nanocubes," *Mater. Lett.*, vol. 60, no. 15, pp. 1896–1900, 2006.

[46] M. N. Owaid, M. A. Rabeea, A. Abdul Aziz, M. S. Jameel, and M. A. Dheyab, "Mushroom-assisted synthesis of triangle gold nanoparticles using the aqueous extract of fresh Lentinula edodes (shiitake), Omphalotaceae," *Environ. Nanotechnology, Monit. Manag.*, vol. 12, no. October, p. 100270, 2019.

[47] J. Xiao and L. Qi, "Surfactant-assisted, shape-controlled synthesis of gold nanocrystals," *Nanoscale*, vol. 3, no. 4, pp. 1383–1396, 2011.

[48] T. Jennings and G. Strouse, "Past, Present, and Future of Gold Nanoparticles," in *Bio-Applications of Nanoparticles* (C. W. C. Warren, ed.), vol. 620, ch. 3, pp. 34–47, Landes Bioscience and Springer Science+Business Media, first ed., 2007.

[49] L. Scarabelli, A. Sánchez-Iglesias, J. Pérez-Juste, and L. M. Liz-Marzán, "A "Tips and Tricks" Practical Guide to the Synthesis of Gold Nanorods," *J. Phys. Chem. Lett.*, vol. 6, pp. 4270–4279, nov 2015.

[50] X. Xu, Y. Zhao, X. Xue, S. Huo, F. Chen, G. Zou, and X. J. Liang, "Seedless synthesis of high aspect ratio gold nanorods with high yield," *J. Mater. Chem. A*, vol. 2, no. 10, pp. 3528–3535, 2014.

[51] Y. Xia, X. Xia, and H. C. Peng, "Shape-Controlled Synthesis of Colloidal Metal Nanocrystals: Thermodynamic versus Kinetic Products," *J. Am. Chem. Soc.*, vol. 137, no. 25, pp. 7947–7966, 2015.

[52] X. Liu, J. Yao, J. Luo, X. Duan, Y. Yao, and T. Liu, "Effect of Growth Temperature on Tailoring the Size and Aspect Ratio of Gold Nanorods," *Langmuir*, vol. 33, no. 30, pp. 7479–7485, 2017.

[53] D. K. Smith, N. R. Miller, and B. A. Korgel, "Iodide in CTAB prevents gold nanorod formation," *Langmuir*, vol. 25, no. 16, pp. 9518–9524, 2009.

[54] A. Gole and C. J. Murphy, "Seed-mediated synthesis of gold nanorods: Role of the size and nature of the seed," *Chem. Mater.*, vol. 16, no. 19, pp. 3633–3640, 2004.

[55] M. J. Walsh, W. Tong, H. Katz-Boon, P. Mulvaney, J. Etheridge, and A. M. Funston, "A Mechanism for Symmetry Breaking and Shape Control in Single-Crystal Gold Nanorods," *Acc. Chem. Res.*, vol. 50, no. 12, pp. 2925–2935, 2017.

[56] S. E. Lohse, N. D. Burrows, L. Scarabelli, L. M. Liz-Marzán, and C. J. Murphy, "Anisotropic noble metal nanocrystal growth: The role of halides," *Chem. Mater.*, vol. 26, no. 1, pp. 34–43, 2014.

[57] N. Garg, C. Scholl, A. Mohanty, and R. Jin, "The role of bromide ions in seeding growth of Au nanorods," *Langmuir*, vol. 26, no. 12, pp. 10271–10276, 2010.

[58] X. Huang, S. Neretina, and M. A. El-Sayed, "Gold nanorods: From synthesis and properties to biological and biomedical applications," *Adv. Mater.*, vol. 21, no. 48, pp. 4880–4910, 2009.

[59] G. Su, C. Yang, and J. J. Zhu, "Fabrication of gold nanorods with tunable longitudinal surface plasmon resonance peaks by reductive dopamine," *Langmuir*, vol. 31, no. 2, pp. 817–823, 2015.

[60] K. Buijs and G. R. Choppin, "Near-Infrared Studies of the Structure of Water. I. Pure Water," *J. Chem. Phys.*, vol. 39, pp. 2035–2041, oct 1963.

[61] N. D. Burrows, S. Harvey, F. A. Idesis, and C. J. Murphy, "Understanding the Seed-Mediated Growth of Gold Nanorods through a Fractional Factorial Design of Experiments," *Langmuir*, vol. 33, no. 8, pp. 1891–1907, 2017.

[62] Personal conversation with Maarten Barnsen, PhD student at the SCM-group, somewhere in the fall of 2021.

[63] M. Bransen, "Synthesis and Self-Assembly of Gold and Gold-Silver Nanorods," p. 89, 2017.

[64] H. G. Hong and W. Park, "Electrochemical characteristics of hydroquinone-terminated self-assembled monolayers on gold," *Langmuir*, vol. 17, no. 8, pp. 2485–2492, 2001.

[65] T.-S. Deng, J. E. S. van der Hoeven, A. O. Yalcin, H. W. Zandbergen, M. A. van Huis, and A. van Blaaderen, "Oxidative Etching and Metal Overgrowth of Gold Nanorods within Mesoporous Silica Shells," *Chem. Mater.*, vol. 27, pp. 7196–7203, oct 2015.

[66] J. Rodríguez-Fernández, J. Pérez-Juste, P. Mulvaney, and L. M. Liz-Marzán, "Spatially-directed oxidation of gold nanoparticles by Au(III)-CTAB complexes," *J. Phys. Chem. B*, vol. 109, no. 30, pp. 14257–14261, 2005.

[67] A. K. Samal, T. S. Sreeprasad, and T. Pradeep, "Investigation of the role of NaBH4 in the chemical synthesis of gold nanorods," *J. Nanoparticle Res.*, vol. 12, no. 5, pp. 1777–1786, 2010.

[68] K. H. Tan, A. Iqbal, F. Adam, N. H. Abu Bakar, M. N. Ahmad, R. M. Yusop, and H. Pauzi, "Influence of Mg/CTAB ratio on the structural, physicochemical properties and catalytic activity of amorphous mesoporous magnesium silicate catalysts," *RSC Adv.*, vol. 9, no. 66, pp. 38760–38771, 2019.

[69] E. Gergely-Fülöp, D. Zámbó, and A. Deák, "Thermal stability of mesoporous silica-coated gold nanorods with different aspect ratios," *Mater. Chem. Phys.*, vol. 148, pp. 909–913, dec 2014.

[70] Y.-S. Chen, W. Frey, S. Kim, K. Homan, P. Kruizinga, K. Sokolov, and S. Emelianov, "Enhanced thermal stability of silica-coated gold nanorods for photoacoustic imaging and image-guided therapy," *Opt. Express*, vol. 18, no. 9, p. 8867, 2010.

[71] R. Zou, Q. Zhang, Q. Zhao, F. Peng, H. Wang, H. Yu, and J. Yang, "Thermal stability of gold nanorods in an aqueous solution," *Colloids Surfaces A Physicochem. Eng. Asp.*, vol. 372, pp. 177–181, dec 2010.

[72] W. C. Wu and J. B. Tracy, "Large-scale silica overcoating of gold nanorods with tunable shell thicknesses," *Chem. Mater.*, vol. 27, no. 8, pp. 2888–2894, 2015.

[73] K. Ma, U. Werner-Zwanziger, J. Zwanziger, and U. Wiesner, "Controlling growth of ultrasmall sub-10 nm fluorescent mesoporous silica nanoparticles," *Chem. Mater.*, vol. 25, no. 5, pp. 677–691, 2013.

[74] N. S. Abadeer, M. R. Brennan, W. L. Wilson, and C. J. Murphy, "Distance and plasmon wavelength dependent fluorescence of molecules bound to silica-coated gold nanorods," *ACS Nano*, vol. 8, no. 8, pp. 8392–8406, 2014.

[75] R. I. Nooney, D. Thirunavukkarasu, Y. Chen, R. Josephs, and A. E. Ostafin, "Self-assembly of mesoporous nanoscale silica/gold composites," *Langmuir*, vol. 19, no. 18, pp. 7628–7637, 2003.

[76] I. Gorelikov and N. Matsuura, "Single-step coating of mesoporous silica on cetyltrimethyl ammonium bromide-capped nanoparticles," *Nano Lett.*, vol. 8, no. 1, pp. 369–373, 2008.

[77] S. Yoon, B. Lee, C. Kim, and J. H. Lee, "Controlled Heterogeneous Nucleation for Synthesis of Uniform Mesoporous Silica-Coated Gold Nanorods with Tailorable Rotational Diffusion and 1 nm-Scale Size Tunability," *Cryst. Growth Des.*, vol. 18, no. 8, pp. 4731–4736, 2018.

[78] J. E. van der Hoeven, H. Gurunarayanan, M. Bransen, D. A. de Winter, P. E. de Jongh, and A. van Blaaderen, "Silica-Coated Gold Nanorod Supraparticles: A Tunable Platform for Surface Enhanced Raman Spectroscopy," *Adv. Funct. Mater.*, vol. 2200148, 2022.

[79] A. H. Bari, R. B. Jundale, and A. Kulkarni, "Understanding the role of solvent properties on reaction kinetics for synthesis of silica nanoparticles," *Chem. Eng. J.*, vol. 398, p. 125427, oct 2020.

[80] "Abel-Ruffini theorem." `https://en.wikipedia.org/wiki/Abel-Ruffini_theorem`. Accessed: 07-12-2022.